Inhibitory Effect of Subthreshold TMS on the Long-Latency Response in the Flexor Carpi Radialis

Cody A. Helm[1], Fabrizio Sergi[1,2]

[1]Department of Biomedical Engineering, University of Delaware, Newark, DE, USA
[2]Department of Mechanical Engineering, University of Delaware, Newark, DE, USA

Correspondence: Fabrizio Sergi (fabs@udel.edu)

Abstract

The corticospinal pathway and several secondary motor pathways contribute to long-latency responses (LLRs). However, it is unknown if secondary pathways can produce LLRs independently from corticospinal input. Transcranial magnetic stimulation (TMS) can modulate corticospinal excitability during the LLR. *Subthreshold* TMS would be ideal for inhibition of corticospinal excitability as it would allow to study function of secondary motor pathways using functional imaging methods with low temporal resolution with minimal activation confound. However, the *subthreshold* TMS parameters that maximally inhibit corticospinal activity are unknown.

In this study, thirty-six healthy participants performed a protocol combining surface electromyography(EMG), robot-evoked wrist perturbations, and single pulse TMS applied to the motor cortex to study the effect of TMS intensity and latency on the LLR amplitude in the flexor carpi radialis. In one experiment, we tested two TMS intensities of 90% and 95% of the active motor threshold and three latencies, defined such that the motor evoked potential (MEP) peak would arrive at 0 ms, 20 ms, or 50 ms prior to perturbation onset (T_1, T_2, T_3, respectively). In a second experiment, we sought to determine whether the inhibitory effect of *subthreshold* TMS was specific to long-latency responses.

TMS significantly reduced the LLR amplitude when applied with T_3 latency,

even when restricting the analysis to stimulation modes that did not induce a motor-evoked response ($p_{adj} = 0.005$). However, we found no evidence that TMS inhibition was specific to the LLR. Overall, our findings indicate that single-pulse, *subthreshold* TMS significantly reduces the corticospinal component of the LLR.

NEW & NOTEWORTHY This study for the first time shows the capability of subthreshold TMS to reduce the long-latency response amplitude in a forearm muscle. We evaluate the effect of the latency between subthreshold TMS and onset of a wrist perturbation using precisely timed TMS pulses, and establish that the inhibition induced by subthreshold TMS is not specific to LLR, but likely resulting from aspecific intracortical inhibition. Insights from this work can be used to design neuroimaging protocols.

Keywords: Transcranial Magnetic Stimulation;Long-Latency Response;Wrist Perturbations;Flexor Carpi Radialis

---

INTRODUCTION

The human neuromuscular system incorporates feedback mechanisms to continuously update movements as we receive new sensory information from our environment. One feedback mechanism is the stretch response which is defined as a burst of EMG activity following an imposed limb displacement (1, 2). An important component of the stretch response is the long-latency response (LLR), which occurs from 50 ms to 100 ms following perturbation onset (3). The LLR occurs between the purely spinal short latency response and the delayed voluntary reaction, each occurring 20 ms to 50 ms and more than 100 ms following perturbation onset, respectively. Notably, the LLR has both spinal and supraspinal components (4, 5, 6).

Multiple motor pathways contribute to the generation of the LLR. A large body of evidence shows that the primary motor pathway, the corticospinal tract (CST), contributes to the long-latency response (4, 7, 5, 8, 9, 3, 6, 10, 1, 11, 12, 13, 14, 15). Strong evidence for the involvement of the CST in the LLR stem from the association between motor cortex neural activity and the long-latency response as well as transcranial magnetic stimulation paradigms (12, 6). Additionally, the reticulospinal tract (RST), a secondary motor pathway, has been suggested to contribute to the long-latency response (16, 17, 18, 19). Extensive research with nonhuman primates has shown the RST to be associated with hand grasping following corticospinal and rubrospinal lesions (20, 21, 22). Excitatory RST connections have been found to attach to hand motoneurons in nonhuman primates and may be as strong as RST connections found in the more proximal muscles (23). In humans, current evidence suggests that the RST is responsible for the increase in the long-latency response when participants are instructed to resist a perturbation rather than yield, highlighting that it contributes to the task-dependent changes (3, 17). Additionally, the StartRe-

act experimental paradigm has shown to elicit a faster than normal planned voluntary muscle activity (∼70 ms post perturbation onset) in the presence of a startling acoustic stimulus prior to a perturbation (24, 25). The decrease in the voluntary response latency is likely contributed by the RST as the only supraspinal pathway able to act with such a short response time (26, 24, 17). Furthermore, a joint perturbation and a startling acoustic stimuli induce a similar EMG recorded response, suggesting that both responses may be generated by the same subcortical pathway (27). Using functional MRI, neural correlates of the LLR were observed in the brainstem during wrist perturbations with the StretchfMRI paradigm (28). These studies provide the muscle-specific brainstem areas associated with the long-latency response and support the notion that the RST contributes to the long-latency response. While our understanding of the motor function of subcortical pathways like the RST is improving, due to limitations in the methods used in previous studies, it is still currently unknown if the RST can generate stretch reflex activity independently from the CST, or if the RST acts solely as a relay for descending CST signal. In the former case, the RST could generate functional motor responses, stretch reflexes, also in absence of CST input. This would support the hypothesis that the RST can provide functional motor responses, regardless of CST input, suggesting its beneficial role in motor recovery in the presence of CST damage. Therefore, alternative methods need to be developed to study the isolated role of the RST on LLR formation, whereby a causal role of this pathway in producing LLR can be identified.

To study the direct role of the RST on the LLR, RST function needs to be decoupled from that of the CST. Transcranial magnetic stimulation (TMS) is a neuromodulation technique that can be used for this purpose. TMS uses a non-invasive time-varying magnetic coil to excite neurons in the line of coil stimulation. When TMS is placed over the motor cortex, motor evoked potentials (MEPs) are measured via surface electromyography of relevant muscles, with a time delay comprised between 10 ms and 30 ms. Following the MEP, there is a decrease in the muscle activity of the targeted muscle which has been referred to as the silent period (29, 30, 31, 32, 33, 34). This TMS-induced silent period has been suggested to last approximately 150 ms to 200 ms, with the first 80 ms of inhibition coming from spinal inhibition and the later part coming from longer lasting cortical inhibition via GABA receptors (34, 35, 36, 37). As such, TMS can modulate the excitability of the corticospinal tract, and thus modulate the contribution of the CST during a stretch-evoked motor response, which would allow to study the contribution of RST to LLRs during reduced CST excitability. With appropriately timed TMS pulses, we can overlay the cortical component of the silent period with the LLR to inhibit its contribution to the long-latency response.

The capability of TMS to inhibit the stretch-evoked long-latency response has been studied under a variety of TMS intensities, latencies between evoked MEP and perturbation onset, and for a variety of tasks. The previous studies that use TMS in the attempt to modulate LLRs are displayed in Fig. S3, broken down by the parameters of TMS stimulation (TMS amplitude and timing), and

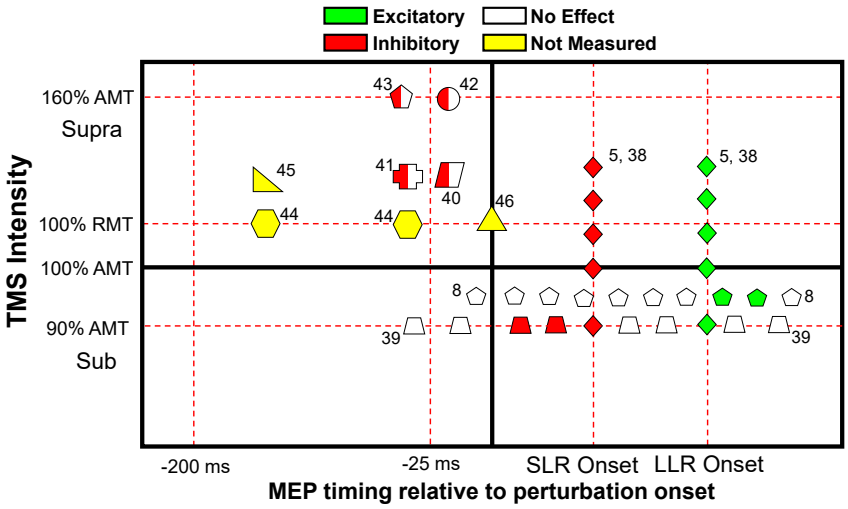

Figure 1: Schematic of previous LLR studies involving TMS. TMS intensity relative to motor threshold is labeled on the y-axis. The timing of the ensuing motor-evoked potential (MEP) relative to perturbation onset is labeled on the x-axis. Each shape corresponds to a different study. Green indicates that the effect of TMS on the LLR was excitatory. Red indicates that the effect of TMS on the LLR was inhibitory. White indicates there was no effect of TMS on the LLR. Yellow indicates the study did not measure the effect of TMS on the LLR.

with an indication of what the measured effects have been.

When applied post perturbation onset, *suprathreshold* TMS (100% - 140% AMT) reduces the LLR amplitude when the MEP peak arrives during the short-latency response onset (38, 5). When *suprathreshold* TMS is timed such that the evoked MEP arrives during long-latency response onset, there is an increase in the EMG response that is greater than the sum of the MEP and LLR alone (38, 5). This demonstrates an increase in the corticospinal tract excitability during the long-latency response. Additionally, when *subthreshold* TMS (96% AMT) is timed such that the ensued motor response arrives 60 ms to 90 ms post perturbation onset, there is an increase in the LLR when the TMS-induced short term facilitatory EMG is overlayed with the long-latency response (8). This shows a sustained involvement of the corticospinal tract on the LLR. Additionally, when *subthreshold* TMS (90% AMT) is applied such that no short-term facilitatory EMG is observed, there is a reduction in the LLR amplitude when applied between 55 ms and 85 ms prior to LLR onset in the tibialis anterior muscle (39).

When timed to arrive prior to perturbation onset, *suprathreshold* TMS (120% resting motor threshold) suppresses the LLR anticipatory modulation associated with a multi-joint dynamic mechanical environment, but does not reduce the LLR amplitude itself (40). Furthermore, at the same TMS timing,

suprathreshold TMS, 120% resting motor threshold, decreases the LLR modulation associated with a task-instruction in the flexor carpi radialis (41). However, previous work also found that a strong *suprathreshold* TMS, mean 160% active motor threshold, arriving prior to perturbation onset reduces LLR modulation associated with the environmental stiffness but does not reduce the LLR modulation associated with task instruction (42, 43). The remaining TMS studies in Figure 1 apply TMS to the motor cortex but do not quantify the excitatory or inhibitory effect of TMS on the LLR amplitude (44, 45, 46).

As far as we know, no studies have investigated the effect of *subthreshold* TMS on the LLR amplitude when the MEP would arrive prior to perturbation onset in the FCR muscle. *Subthreshold* TMS would be beneficial as it reduces the excitatory effect of TMS stimulation on the motor cortex regions, as would be observed with *suprathreshold* TMS, which further highlights the inhibitory effect of TMS. Additionally, *subthreshold* TMS timed such that the MEP would arrive prior to perturbation onset would properly engage the cortical, and not spinal, component of the TMS-evoked silent period during the LLR. It remains unknown whether *subthreshold* TMS when the MEP would arrive prior to perturbation onset can significantly reduce the LLR amplitude via the cortical component of the silent period. Additionally, the distinct *subthreshold* TMS stimulation intensity and latency that result in the maximal reduction of the cortical contribution, via the silent period, to the LLR of the FCR muscle are unknown. Furthermore, it is unknown whether the inhibitory effect induced by *subthreshold* would be specific to LLRs, or would be measured also in absence of applied muscle stretch.

The objective of this study was to determine whether *subthreshold* TMS can significantly reduce the CST's contribution to the LLR in a forearm flexor muscle, FCR, and to investigate the optimal TMS intensity and timing that would maximally inhibit the amplitude of LLRs evoked via controlled perturbation of the wrist. A secondary goal of this study was to establish whether the TMS-induced inhibition is specific to LLR, or if a similar inhibition is also measured in absence of applied muscle stretch. The outcomes of this study provide insight into the mechanisms by which *subthreshold* TMS results in inhibition of the LLR and the specific *subthreshold* TMS intensity and latency needed to overlay the cortical component of the EMG silent period with the LLR in the forearm. The knowledge from this study may be used to study the role of subcortical or spinal mechanisms in both the generation and the modulation of the long-latency response during reduced corticospinal tract signal.

MATERIALS AND METHODS

Participants

36 healthy participants (21 male/15 female, age range: 19–39 years) performed the experimental protocol. The subjects were divided evenly into three groups (n=12), each exposed to different TMS modes. All of the subjects were right-handed and free from neurological disorders and did not have any contra-

indications to MRI or TMS. The subjects provided informed written consent for the study. The study was approved by the Institutional Review Board of the University of Delaware (IRB no: 1545543-5, -6, -7, and -8) and was in accordance with the Declaration of Helsinki.

Experimental Setup

In this study, we combined a wrist robot, the MR-StretchWrist, used to elicit stretch reflexes in the forearm, with TMS, used to stimulate the motor cortex with precise timing, and surface EMG, used to record muscle activity in one forearm muscle. Details on these elements are provided below.

Surface Electromyography

Bi-polar surface electrodes were placed on the skin over the flexor carpi radialis (FCR) to record muscle activity. The location of the FCR muscle belly was determined by having the subject flex and relax their wrist and palpating down the forearm muscle. The skin was cleaned with a 70% Isopropyl alcohol wipe (Med Price) to remove any dirt and debris on the surface of the forearm. A thin layer of skin was abraded with Nuprep skin prep gel (Weaver and Company) to reduce contact impedance. The electrodes (standard multitrode Ag/AgCl bipolar electrodes from Brain Products, Munich, Germany) were firmly attached on the skin surface using double-sided adhesive collars (BIOPAC Systems, Inc.). The bi-polar electrodes were aligned with the direction of the muscle fibers. An additional electrode (ground electrode) was placed on the olecranon in the back of the elbow to serve as a ground. Each electrode was filled with a high-chloride abrasive electrolyte gel (EASYCAP) to further reduce contact impedance. Muscle activity was amplified using an 8-channel bipolar amplifier (MR Plus ExG, BrainVision, Munich, Germany). Muscle signal and external triggers were synced together using a Trigger and Sync Box (BrainVision). The EMG signal was filtered with a 60 Hz notch filter and visualized and recorded using BrainVision Recorder software. Proper electrode placement was confirmed by having the subject perform flexion and radial deviation contractions and observing a high signal to noise ratio in agonist muscles.

Robotic perturbations

We used the MR-StretchWrist to apply perturbations and evoke stretch reflexes on forearm muscles. The MR-StretchWrist is an MRI-compatible wrist robot previously developed by the Human Robotics Lab (28) at the University of Delaware uses a piezoelectric ultrasonic motor to apply velocity-controlled perturbations to the wrist joint and an incremental encoder to continuously measure wrist angle. The MR-StretchWrist incorporates a force/torque sensor to measure wrist torques applied by the subject. During a wrist perturbation, a velocity command of 150°/sec is sent to the MR-StretchWrist for 200 ms in the extension direction to elicit a stretch reflex response in wrist flexors, including

the FCR muscle. Following perturbations, the wrist robot returns the wrist to the neutral posture at a slow velocity (35°/s) to avoid eliciting a stretch reflex.

Transcranial Magnetic Stimulation

A neuronavigation procedure was performed to position the TMS coil over the participant's forearm motor hotspot of the motor cortex. First, the participant's structural brain scan was loaded into the Neuronavigation software (Localite 3.3.0). With the Localite software, brain segmentation was performed to virtually extract a 3d rendering of the brain volume from the skull. We converted from subject space to Talairach space by manually defining the anterior commissure, posterior commissure, and cortical falx point on the brain scan. A target marker was placed on the forearm motor hotspot of the motor cortex as the location that we aimed to stimulate with TMS. The target marker was defined visually by identifying the pre-central gyrus, and then moving laterally along the gyrus until reaching the hotspot for muscles responsible for movements of the distal upper extremity. An entry marker was placed on the surface of the skull that the TMS coil would be positioned. The entry marker was oriented approximately 45° from the mid-sagittal line for adequate target stimulation to occur (47).

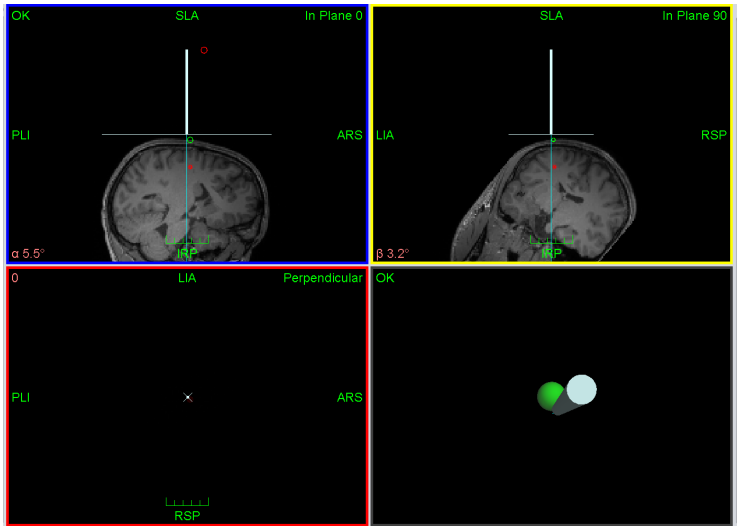

Figure 2: Localite Neuronavigation software displaying the position and orientation of the TMS coil (blue line) and the position of the entry marker (green circle) and target marker (red circle) for accurate coil placement. Blue box displays the sagittal plane and the yellow box displays the coronal plane. The bottom right box displays the plane looking down on the entry-target axis and the red box displays the plane perpendicular to the entry-target axis plane.

Next, we performed subject registration to register the physical features of

the subject's head with the Neuronavigation system. We used motion capture tracking and reflective markers to register the position and orientation of the subject's head and TMS coil in 3D space. A figure-of-eight TMS coil (MCF-B65, Magventure) was calibrated to the camera which defined the position and orientation of the center of TMS coil relative to the coil's markers. We placed reflective markers on the subject's forehead via double-sided skin adhesive tape for subject registration. Subject registered included a 'landmark registration' and a 'surface registration'. For 'landmark registration', the 'left tragus', 'right tragus', and 'nasion point' were manually defined on the brain scan. A pointer was used to calibrate the features of the subject's head with the respective markers on the brain scan. During 'surface registration', a pointer was moved across the surface of the subject's head to collect a minimum of 200 points to calibrate the surface of the subject's head with the TMS software. The landmark and surface registration steps were verified by comparing the positions of the landmarks and surfaces in real space with the respective locations on the virtual brain scan. A root mean squared error of less than 4.0 mm was considered acceptable for coil placement.

Following the Neuronavigation procedure, a chin support connected to the procedural chair was locked in place to support the subject's head and minimize head movement throughout the experiment. The TMS coil was placed over the forearm motor hotspot of the subject using the Neuronavigation system. Proper placement of the TMS coil was confirmed by sending three TMS pulses to the motor cortex (intensity: 80%) and observing whether motor evoked potentials were present. If there were no motor evoked potentials, the TMS coil was repositioned until motor evoked potentials were observed. The TMS stimulator (MagPro X100, Magventure) settings were set to biphasic waveform, twin pulse mode, and normal current direction for all the TMS pulse stimulations.

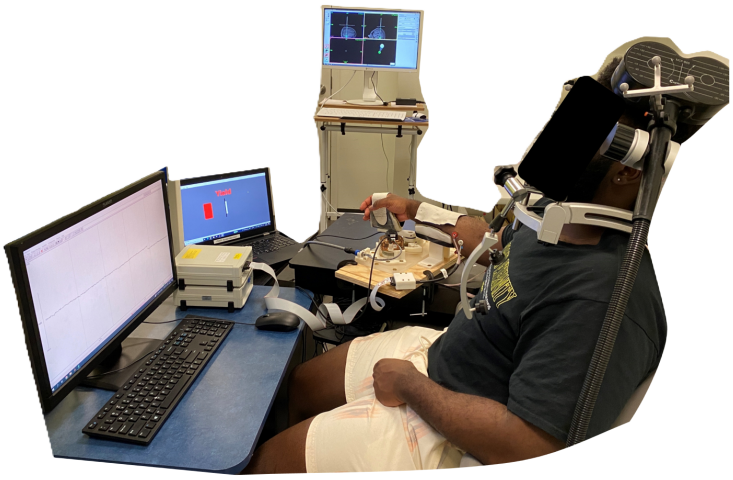

Figure 3: Laboratory experimental setup with the TMS system, MR-StretchWrist robot, and FCR surface EMG acquisition. The TMS coil is placed on the surface of the head and directed towards the forearm motor hotspot area. Accurate placement of the TMS coil is confirmed with the TMS neuronavigation software, Localite.

Procedures

MRI Structural Scan

During a first visit, we acquired a high-resolution structural brain scan for each subject using a Siemens 3T MRI scanner (Center for Biomedical & Brain Imaging, University of Delaware). Subjects were screened with an MRI safety screening form to ensure they were safe to be scanned in the MRI. The subject laid in the supine position on the scanner bed and was instructed to relax and minimize movement during the scan. The high resolution T_1 MP-RAGE structural scan required a total of 30 minutes to perform with a 0.7x0.7x0.7mm^3 voxel resolution, TR = 2300 ms, TE = 3.2 ms and 160 slices with 256 x 256 px per image.

Active Motor Threshold and T_{MEP} Determination

Once it was confirmed that the TMS was placed over the forearm hotspot of the left motor cortex, we determined the subject specific active motor threshold (AMT) and T_{MEP} latency. The AMT was defined as the minimum TMS intensity that elicited at least 5 out of 10 motor evoked potentials (MEPs) when the muscle was in the target activation state. A MEP was recorded if the measured EMG response exceeded a threshold of 200 μV. The subject was cued to maintain a wrist flexion torque of 0.3 Nm as indicated by a visual display. The visual

display was composed of a horizontal bar whose length was mapped to the measured wrist flexion torque, and whose color changed from gray to green if the measured torque was within 0.07 Nm of the target. Once participants matched the target torque, a train of TMS stimuli was applied. Ten single pulse stimuli were fired manually at each intensity, with an approximate inter-stimulus time of 5 s, and the number of MEPs that crossed the threshold were counted. The subject was cued to relax following the 10 stimuli. The TMS stimulus intensity started at 40% of the maximum stimulation output (MSO) of the TMS stimulator. If the number of MEPs recorded at a given amplitude was below 5, the intensity was increased by 10% until the number of MEPs was equal to or greater than 5. The stimulus intensity was then decreased by 5%, then changed by 2% until we found the lowest TMS intensity that yielded at least 5 MEPs. The measured value of AMT was used to define stimulation amplitudes in the later portion of the experiment. TMS timing were calculated for the later portions of the experiment based on the subject's T_{MEP} latency. The T_{MEP} latency was defined as the average delay between the time the TMS was fired and the absolute maximum or minimum of the measured EMG track. T_{MEP} was determined by pooling together the EMG responses elicited by supra-threshold stimuli at the subject's AMT.

Experiment 1 Task

In the task, the MR-StretchWrist robot was used to elicit stretch reflexes in forearm muscles, TMS was used to stimulate the left motor cortex in proximity of the motor hotspot for muscles in the right forearm, and FCR muscle activity was recorded using sEMG. Perturbations were applied to the wrist joint in the extension direction to elicit a stretch response in the FCR muscle. To study the effect of *subthreshold* TMS intensity on the LLR amplitude, two *subthreshold* TMS intensities were employed in the study, with two levels (i.e., 90% AMT and 95% AMT). Each group was exposed to one TMS intensity, i.e. Group 1 was exposed to the 90% AMT intensity, and Group 2 was exposed to the 95% AMT intensity. Within each group, TMS pulses were applied with three different latencies ΔT relative to perturbation onset. The latencies were computed such that the MEP would peak T_L ms before perturbation onset (see Fig. 3). In our study, we investigated three levels for MEP latency T_L, with T_1=0 ms, T_2=20 ms, T_3=50 ms. Latencies were applied such that the ensuing silent window, supposed to be of approximately 150 ms of duration (31, 34), would completely overlap with the LLR portion of the stretch-evoked response.

In addition to the three TMS latency modes, we applied stimuli using two additional control mode, one (Pert), where perturbations were applied in absence of TMS, and one (Back Only), where no perturbations nor TMS were applied after the subject matched the torque target. There was a total of 20 trials per mode throughout the experiment for a total of 100 trials. The order of modes was randomized through the experiment at the individual trial level. Prior to the experiment, participants were instructed to yield to the perturbation (when applied) as soon as they felt the robot began to perturb them.

Each trial began by cueing the participant to maintain a wrist flexion torque of 0.3 Nm as indicated by a visual display, just like in the AMT session. Upon matching the torque target, the TMS stimulus would be applied at a random point normally distributed between 400 and 800 ms. Following perturbation, the robot would return the wrist to the neutral position at a low velocity, and the target bar for the next trial would appear after a delay ΔT calculated from a uniform distribution $\mathcal{U}_{[a,b]}$ with $a = 3$ s and $b = 7$ s.

Experiment 2 Task

To quantify the effect of single pulse *subthreshold* TMS stimulation on voluntary activation measured in absence of imposed stretch, and compare this effect with the TMS-induced LLR inhibition, we performed a second experiment with N=12 participants. The TMS intensity selected was 90% active motor threshold. We applied the Back mode, Pert mode, and Perturbation with TMS with a latency of T_3 similar to the first experiment. In addition, we included a TMS with background mode, where TMS was applied during active background contraction without a perturbation present. Each mode was repeated 25 times in a randomized order as an event-related design for a total of 100 trials.

Due to the AMT determined in experiment 1 being larger than those previously reported in the literature (5, 42, 8), we slightly modified the TMS coil orientation to conform with previously reported procedures. All TMS pulses for experiment 2 were applied at a coil orientation of 45° relative to the mid-sagittal plane, oriented in the posterior-anterior direction (PA). This TMS coil orientation has been shown to be the most effective in eliciting motor evoked responses at lower TMS intensities compared to other orientations (48), and can thus be considered the gold standard for excitatory TMS paradigms.

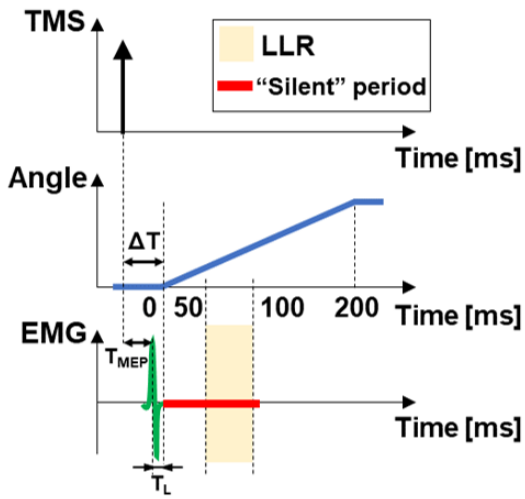

Figure 4: TMS timing diagram showing the synchronization of TMS pulse application, wrist perturbation, expected flexor carpi radialis muscle activity response, and silent period. T_L is the timing of the peak of the MEP relative to perturbation onset for a *suprathreshold* MEP response condition. The expected muscle activity response is in the case of a *suprathreshold* motor evoked potential.

Data Analysis

EMG

Raw EMG data was acquired for the FCR muscle for all 100 experimental trials and digitized using the EMG amplifier. The digitized EMG data was filtered with a 60 Hz notch filter. Then, the EMG signal was filtered by applying a fourth order bandpass filter with a high pass frequency of 20 Hz and a low pass frequency of 500 Hz. Then, the EMG response was subject to full-waved rectification by taking the absolute value of the EMG. Finally, the rectified EMG response was filtered with a fourth order low pass frequency of 60 Hz. Background EMG activity was defined as filtered EMG activity from 100 ms to 50 ms prior to perturbation onset. For a given trial, filtered EMG activity from 100 ms prior to perturbation onset to 150 ms post perturbation onset was subject to statistical analysis. The filtered EMG activity was normalized for each trial by dividing it by the average background activity of all trials. Thus, the normalized EMG response in normalized units (n.u.) were obtained for each trial. For each trial, the normalized EMG response from 50 ms to 100 ms was averaged to obtain the LLR amplitude (LLRa).

EMG Data Exclusion by Motor Evoked Potential

Due to the focus of this study on quantifying the effect of subthreshold TMS stimulation, EMG signal measured in all TMS active conditions was screened to establish whether a motor evoked potential (MEP) was indeed evoked. To do so, trials were labeled as MEP positive ($\text{MEP}^{(+)}$) if the peak of the EMG signal during the expected motor evoked potential window was greater than 1 times the standard deviation of the distribution of peak background EMG signal of the rectified EMG measured prior to a perturbation. Trials where the EMG peak was below the threshold were considered $\text{MEP}^{(-)}$. Trial exclusion was performed on an individual subject basis. To evaluate the sensitivity of the results to a somewhat arbitrary threshold, the operation of labeling as $\text{MEP}^{(+)}$ or $\text{MEP}^{(-)}$ was repeated using different criteria, where the threshold reported above was changed from 1x the standard deviation to: a) 2x the standard deviation; b) 3x the standard deviation; c) 200 μV, d) the median of the evoked MEPs for that participant.

This EMG data exclusion method was used for statistical analysis of both experiments 1 and 2.

We applied additional MEP thresholding methods to determine whether the results changed with different criteria for defining a motor evoked potential. For the 200 μV thresholding, trials were excluded if the peak EMG signal during the MEP window exceeded 200 μV. For the median threshold, trials with EMG peaks during the MEP window that were greater than the median EMG peak were excluded. We implemented a 2x standard deviation threshold and a 3x standard deviation threshold in respect to the background EMG signal and if the EMG peak went above the threshold we excluded those trials.

Statistical Analysis

Subject Specific Stimulation Parameters

We performed a 1-way repeated measures ANOVA to compare the active motor threshold intensities and T_{MEP} between the three TMS groups, as we wanted to verify that there were no significant differs between the active motor thresholds and the MEP latencies between the groups. Post-hoc analysis was performed using Tukey HSD all pairwise comparisons on effects that were significantly different.

Experiment 1

Group Analysis

We performed a linear mixed model to determine the effects of TMS latency and intensity on the LLR amplitude. Outliers were removed by subject using the Huber Method with an outlier threshold equal to 4 standard deviations from the mean, for each subject. In the model, the fixed effects were TMS mode (5 levels: T_1, T_2, T_3, TMS off - Pert On, Background Only), TMS intensity (2 levels: 90% of AMT and 95% of AMT) and the interaction between TMS mode

and intensity. The linear mixed model included random effects of subject and subject·TMS mode. The mixed model accounted for unequal variance between different TMS modes and subjects. In presence of a significant fixed effect, post-hoc analysis was performed using Dunnett's test for multiple comparisons with control to determine which TMS modes were significantly different from the control mode of TMS off - Pert On. An α threshold value of 0.05 was used to determine statistical significance. We quantified the percent change in the perturbation due to TMS as the difference between the LLRa in the control mode compared to the TMS mode, divided by the LLRa in the control mode.

An additional analysis was performed using separate linear mixed models for each TMS intensity to determine the effect of TMS mode for each TMS intensity group (90% or 95% active motor threshold). The linear mixed model included fixed effects of TMS mode, and random effects of subject and subject · TMS mode. The mixed model accounted for unequal variance between different TMS modes and subject. In presence of a significant fixed effect, post-hoc analysis was performed using Dunnett's test for multiple comparisons with control to determine if any TMS mode was significantly different from the control mode (TMS off - Pert On). øincrease specificity to only subthreshold TMS events, we performed the same linear mixed models as stated above but only data from $\text{MEP}^{(-)}$ trials.

Sensitivity of the Results to MEP Definition Threshold

We applied the same linear mixed model reported above using different thresholding methods for the identification of $\text{MEP}^{(-)}$ trials, while only including data from the identified $\text{MEP}^{(-)}$ trials. The linear mixed model had the fixed effect of TMS mode for T_3 with random effects of subject ID and subject ID · TMS mode, with unequal variances between TMS modes. Post-hoc analysis was used to determine which TMS modes were significantly different than the control mode: Pert.

Supplementary Analyses

Subject-specific analysis was performed to determine which TMS modes had a significant effect on the LLRa for each subject. This allowed us to determine for which subjects TMS had a significant effect on the LLRa and for TMS modes resulted in a significant reduction in the LLRa. Additionally, we were interested in evaluating the effect of TMS over the entire EMG time series and we conducted a 1-D time series analysis to determine the effect of TMS on the entire EMG time series. We have included the subject specific analysis and time series analysis on the TMS experiment 1 data in the supplementary materials.

Experiment 2

Group analysis

We used a linear mixed model to determine the effects of MEP type and perturbation on the LLR amplitude. In the model, the fixed effects were Pert mode (2 levels: 0 and 1 for perturbation off and on, respectively), MEP type (3 levels: $\text{TMS}^{(-)}$, $\text{MEP}^{(-)}$, and $\text{MEP}^{(+)}$) and the interaction between Pert mode and MEP type. The linear mixed model included random effects of subject,

subject·Pert mode, and subject·MEP type. The mixed model accounted for unequal variance between subjects. In presence of a significant fixed effect, post-hoc analysis was performed using Dunnett's test for multiple comparisons with control to determine which MEP types were significantly different from the control for both Pert on and Pert off. An α threshold value of 0.05 was used to determine statistical significance.

RESULTS

Subject Specific Stimulation Parameters

The distribution of subject-specific stimulation parameters are reported in Fig. 5. The AMT values were found to be significantly different between groups ($F = 8.812$, $df = 2$, $p < 0.001$). Average AMT was 71.8 (±12.6 s.d.) %MSO, 65.7 (±10.3 s.d.) %MSO, and 53.9 (±8.5 s.d.) %MSO for the 90% AMT, 95% AMT, and Exp2 groups, respectively.

Post hoc analysis showed that the 90 and 95 groups were significantly different from the Exp2 group but not from each other (mean ± s.e.m. of the difference – 90 − 95: 6.167 ± 4.336 %MSO, $p_{adj} = 0.341$; 90-Exp2: 17.91 ± 4.336 %MSO, $p_{adj} < 0.001$; 95-Exp2: 11.75 ± 4.336 , $p_{adj} = 0.028$).

We found no significant difference in the T_{MEP} latency values between the three groups ($F = 1.824$, $df = 2$, $p = 0.177$). The average T_{MEP} latency was 26.8 ms ± 8.0 ms, 30.6 ms ± 5.5 ms, and 31.5 ms ± 5.6 ms for the 90% AMT, 95% AMT, and Exp2 groups, respectively.

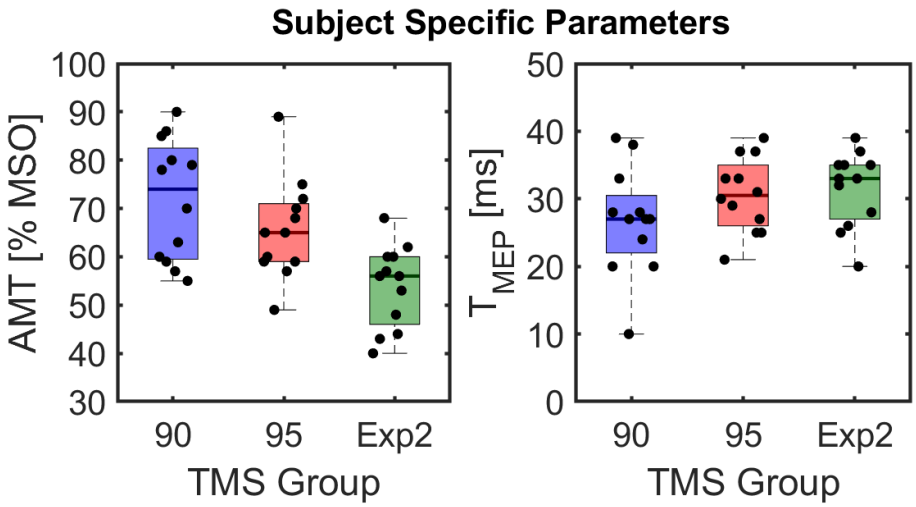

Figure 5: Distribution of active motor threshold and T_{MEP} latency measurements for each group. Solid black lines inside the boxplot indicate median, boxplot boundaries indicate 25% and 75% IQR and outer lines indicate min and max data points. AMT and T_{MEP} values for each subject are denoted with black dots.

Experiment 1

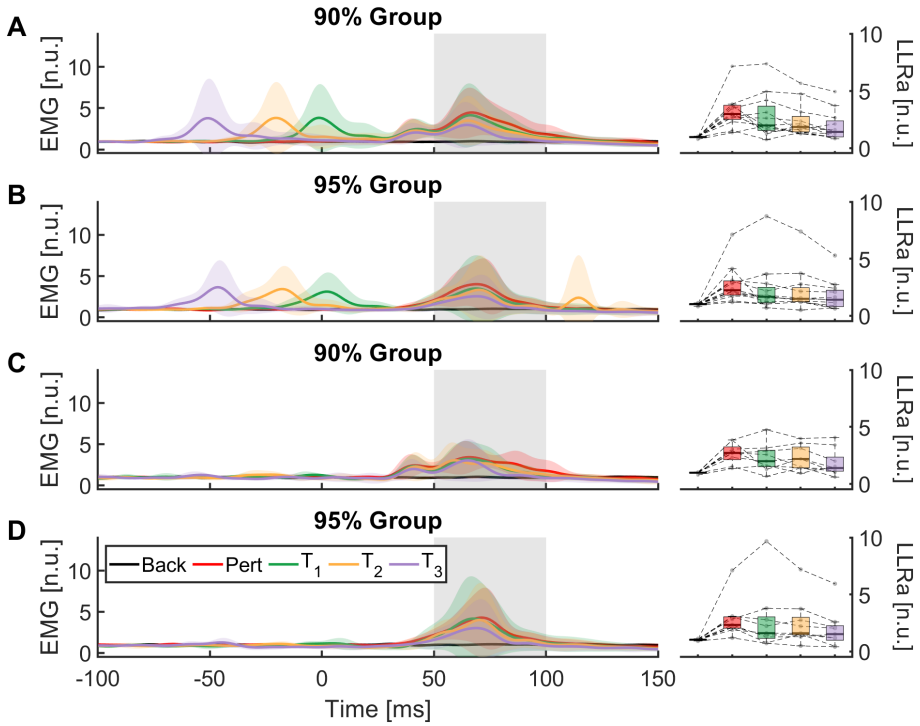

Figure 6: (Left) Experiment 1 normalized EMG Plots. Group mean normalized EMG responses for each TMS mode are displayed from -100 ms to 150 ms relative to perturbation onset, and a shaded area indicates ± one standard deviation for that group. (Right) The long latency response amplitudes (LLRa) for each TMS mode are displayed and broken down by TMS group. Each dot denotes the within subject average for that TMS mode. The middle line is the median of the distribution with the box ends indicating the 25% - 75% IQR. Whiskers extend out to the furthest datapoint that is not considered an outlier. A/B: Normalized EMG time series data for all trials. C/D: Normalized EMG time series data excluding $\text{MEP}^{(+)}$ trials.

Group-level analysis

Experiment 1 EMG time series data and subject specific LLRa are reported in Fig. 6. Based on the two-way linear mixed model, TMS mode had a significant effect on the normalized LLRa ($F = 16.85$, $df = 96.0$, $p_{adj} < 0.001$), as shown in Table 1. No significant effect was found for the effect of TMS intensity nor TMS intensity·mode ($F = 0.196$, $df = 22.0$, $p_{adj} = 0.6624$; $F = 0.228$, $df = 96.0$, $p_{adj} = 0.9218$, respectively). Post-hoc analysis performed using the Dunnett's method with control showed that T_2, T_3, and the Back Only modes

were significantly different compared to the Pert mode (mean ± s.e.m. of the difference – T_2−P: -0.694 ± 0.263 n.u., $p_{adj} = 0.0330$; T_3−P: -1.09 ± 0.261 n.u., $p_{adj} < 0.001$; BO−P: -1.92 ± 0.254 n.u., $p_{adj} < 0.001$), while T_1 was not (T_1−P: -0.412 ± 0.264 n.u., $p_{adj} = 0.333$).

For the 90% AMT group, the linear mixed model showed that TMS mode had a significant effect on the normalized LLRa ($F = 11.5$, $df = 49.7$, $p_{adj} < 0.001$). Post-hoc analysis performed using the Dunnett's method with control showed that the T_3 and the Back Only modes were significantly different compared to the Pert mode (T_3-P: -1.18 ± 0.356 n.u., $p_{adj} = 0.0063$; BO-P: -2.156 ± 0.343 n.u., $p_{adj} < 0.001$), while T_1 and T_2 were not (T_1-P: -0.483 ± 0.358 n.u., $p_{adj} = 0.4643$; T_2-P: -0.817 ± 0.358 n.u., $p_{adj} = 0.085$), as shown in Fig. 7.

For the 95% AMT group, the linear mixed model showed that TMS mode had a significant effect on the normalized LLRa ($F = 6.1$, $df = 46.6$, $p_{adj} < 0.001$). Post-hoc analysis using the Dunnett's method with control showed that the T_3 and the Back Only modes were significantly different compared to the Pert mode (T_3-P: -1.01 ± 0.383 n.u., $p_{adj} = 0.0386$; BO-P: -1.692 ± 0.375 n.u., $p_{adj} < 0.001$, respectively), while T_1 and T_2 were not (T_1-P: -0.342 ± 0.387 n.u., $p = 0.7881$; T_2-P: -0.572 ± 0.385 n.u., $p = 0.3843$), as shown in Fig. 7.

Based on the two-way linear mixed model for $MEP^{(-)}$ trials, TMS mode had a significant effect on the normalized LLRa ($F = 15.38$, $df = 84.3$, $p_{adj} < 0.001$), as shown in Table 2. No significant effect was found for the effect of TMS intensity nor TMS intensity · mode ($F = 0.08$, $df = 23.7$, $p_{adj} = 0.774$; $F = 0.78$, $df = 84.3$, $p_{adj} = 0.544$, respectively). Post-hoc analysis performed using the Dunnett's method with control showed that T_3 and the Back Only modes were significantly different compared to the Pert mode (T_3−P: -1.05 ± 0.317 n.u., $p_{adj} = 0.005$; BO-P: -1.994 ± 0.269 n.u., $p_{adj} < 0.001$), while T_1 and T_2 were not (T_1−P: -0.410 ± 0.330 n.u., $p_{adj} = 0.562$; T_2−P: -0.657 ± 0.324 n.u., $p_{adj} = 0.150$).

Following $MEP^{(+)}$ exclusion, 3 participants in the 90% AMT group had low to no $MEP^{(-)}$ trials and were removed from the plot. For the 90% AMT group with only the $MEP^{(-)}$ trials, the linear mixed model showed that TMS mode had a significant effect on the normalized LLRa ($F = 11.63$, $df = 37.0$, $p_{adj} < 0.001$). Post-hoc analysis performed using the Dunnett's method with control showed that T_2, T_3, and the Back Only modes were significantly different compared to the Pert mode (T_2−P: -1.130 ± 0.396 n.u., $p_{adj} = 0.025$; T_3−P: -1.39 ± 0.376 n.u., $p_{adj} = 0.003$; BO-P: -2.248 ± 0.334 n.u., $p_{adj} < 0.001$), while T_1 was not (T_1−P: -0.972 ± 0.402 n.u., $p_{adj} = 0.069$), as shown in Fig. 7.

Following $MEP^{(+)}$ exclusion, 4 participants in the 95% AMT group had low to no $MEP^{(-)}$ trials and were removed from the plot. For the 95% AMT group with only the $MEP^{(-)}$ trials, the linear mixed model showed that TMS mode had a significant effect on the normalized LLRa ($F = 5.75$, $df = 42.7$, $p_{adj} < 0.001$). Post-hoc analysis using the Dunnett's method with control showed that the Back Only mode was significantly different compared to the Pert mode (BO-P: -1.740 ± 0.417 n.u., $p_{adj} < 0.001$, respectively), while T_1, T_2, and T_3 were not (T_1−P: 0.096 ± 0.525 n.u., $p = 0.999$; T_2−P: -0.224 ± 0.512 n.u., $p = 0.981$; T_3−P: -0.741 ± 0.515 n.u., $p = 0.440$), as shown in Fig. 7.

Fixed Effect	DFNum	DFDen	F Ratio	p-value
TMS Mode	4	96	16.85	<0.001
Intensity	1	22.0	0.196	0.662
TMS Mode·Intensity	4	96	0.228	0.922

Table 1: In TMS Experiment 1, the linear mixed model results for the two-way ANOVA test for all trials.

Fixed Effect	DFNum	DFDen	F Ratio	p-value
TMS Mode	4	84.3	15.38	<0.001
Intensity	1	23.7	0.08	0.774
TMS Mode·Intensity	4	84.3	0.78	0.544

Table 2: In TMS Experiment 1, the linear mixed model results for the two-way ANOVA test for MEP$^{(-)}$ trials.

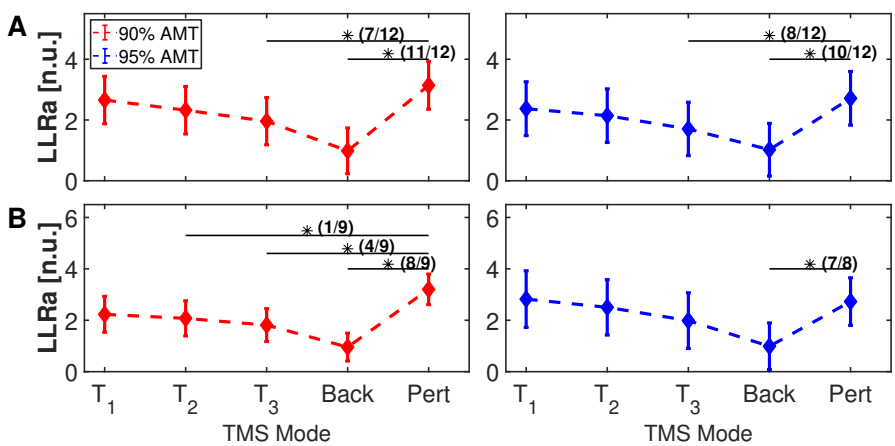

Figure 7: Effect of TMS mode on the long latency response amplitude (LLRa) broken down by TMS intensity (i.e., group). Asterisks denote significant effects within each group, and numbers in parenthesis indicate the number of subjects for which that effect was detected as significant. A: LLR amplitude from all trials. B: LLR amplitude data from only MEP$^{(-)}$ trials.

Sensitivity of Results to MEP Threshold Definition

The presence of an inhibitory effect of TMS in MEP$^{(-)}$ trials was consistently highlighted regardless of the choice of a specific thresholding method, in the T_3 mode, as shown in Fig. 8. Specifically, a significant difference between Pert On and MEP$^{(-)}$ was measured for all thresholding methods (3X SD: MEP$^{(-)}$−P: -1.054 ± 0.270 n.u., $p_{adj} < 0.001$; 2X SD: -1.006 ± 0.278 n.u., $p_{adj} = 0.002$; 1X

SD: -1.042 ± 0.290 n.u., $p_{adj} = 0.002$; Median: -1.157 ± 0.258 n.u., $p_{adj} < 0.001$; 200μV: -1.148 ± 0.262 n.u., $p_{adj} < 0.001$). A significant difference between Pert On and MEP$^{(+)}$ was also measured for all thresholding methods (3X SD: MEP$^{(+)}$–P: -1.205 ± 0.286 n.u., $p_{adj} < 0.001$; 2X SD: -1.157 ± 0.277 n.u., $p_{adj} < 0.001$; 1X SD: -1.081 ± 0.264 n.u., $p_{adj} < 0.001$; Median: -1.123 ± 0.252 n.u., $p_{adj} < 0.001$; 200 μV: -1.102 ± 0.309 n.u., $p_{adj} = 0.002$).

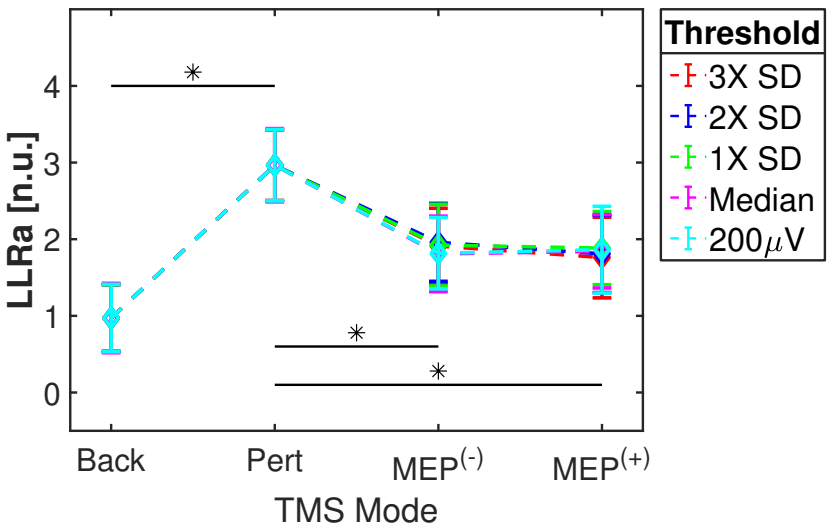

Figure 8: Experiment 1 Mixed Model results at TMS latency set to T_3 with different MEP peak thresholding methods. Effects of TMS mode on the long latency response amplitude (LLRa) pooled in both groups. Asterisks denote significant effects at the group level and they are consistent across all thresholding methods.

Experiment 2

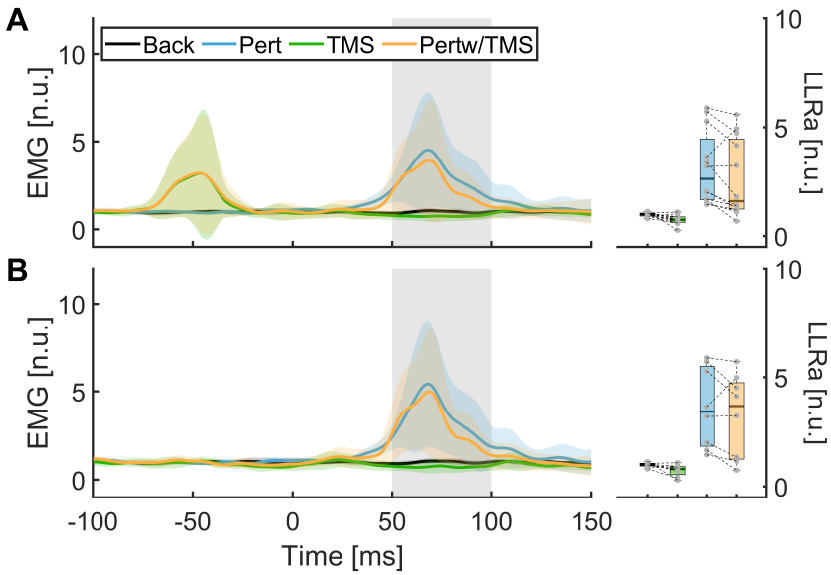

Figure 9: (Left) Experiment 2 normalized EMG Plots. Group mean normalized EMG responses for each TMS mode are displayed from -100 ms to 150 ms relative to perturbation onset, and a shaded area indicates the ± one standard deviation for that group. (Right) The LLR amplitudes for each TMS mode are displayed and broken down by TMS group. Each dot denotes the within subject average for that TMS mode. The middle line is the median of the distribution with the box ends indicating the 25% - 75% IQR. Whiskers extend out to the furthest datapoint that is not considered an outlier. A: Normalized EMG time series data for all trials. B: Normalized EMG time series data for only $\text{MEP}^{(-)}$ trials.

Group-level analysis

Following $\text{MEP}^{(+)}$ exclusion, 4 participants in the Exp2 group had low to no $\text{MEP}^{(-)}$ trials and their data were removed. Experiment 2 EMG time series data and subject specific LLRa are reported in Fig. 9. The linear mixed model identified a significant effect of Pert mode and MEP Type on the normalized LLRa ($F = 17.58$, $df = 10.8$, $p_{adj} = 0.002$; $F = 6.10$, $df = 15.9$, $p_{adj} = 0.0108$, respectively), as well as their interaction ($F = 8.344$, $df = 591.5$, $p_{adj} < 0.001$), see Table. 3. Post-hoc analysis performed using the Dunnett's method with control showed that $\text{MEP}^{(-)}$ and $\text{MEP}^{(+)}$ trials were significantly different than $\text{TMS}^{(-)}$ trials for Pert On (Pert_1: $\text{MEP}^{(-)}-\text{TMS}^{(-)}$: -0.402 ± 0.145 n.u., $p_{adj} = 0.0209$; $\text{MEP}^{(+)}-\text{TMS}^{(-)}$: -0.523 ± 0.124 n.u., $p_{adj} < 0.001$), whereas $\text{MEP}^{(-)}$ and $\text{MEP}^{(+)}$ trials were not significantly different than $\text{TMS}^{(-)}$ trials for Pert Off (Pert_0: $\text{MEP}^{(-)}-\text{TMS}^{(-)}$: -0.287 ± 0.146 n.u., $p_{adj} = 0.161$;

$\text{MEP}^{(+)}-\text{TMS}^{(-)}$: -0.218 ± 0.124 n.u., $p_{adj} = 0.246$), see Fig.10.

The difference in LLR between $\text{TMS}^{(-)}$ and $\text{MEP}^{(-)}$ was not significantly different in the Pert On condition, relative to the Pert Off condition ($(\text{TMS}^{(-)} - \text{MEP}^{(-)})_{\text{Pert}_1} - (\text{TMS}^{(-)} - \text{MEP}^{(-)})_{\text{Pert}_0}$) : 0.064 $\pm$0.077 n.u., $p_{adj} = 0.404$), suggesting lack of specificity of the effects with regards to stretch-evoked responses. The difference in LLR between $\text{TMS}^{(-)}$ and $\text{MEP}^{(+)}$ was significantly different in the Pert On condition, relative to the Pert Off condition ($(\text{TMS}^{(-)} - \text{MEP}^{(+)})_{\text{Pert}_1} - (\text{TMS}^{(-)} - \text{MEP}^{(+)})_{\text{Pert}_0}$: 0.1884 $\pm$0.070 n.u., $p_{adj} = 0.007$).

Fixed Effect	DFNum	DFDen	F Ratio	p-value
Pert Mode	1	10.8	17.58	0.002
MEP Type	2	15.9	6.101	0.011
Pert Mode·MEP Type	2	591.5	8.344	<0.001

Table 3: In TMS Experiment 2, the Linear Mixed Model results for the two-way ANOVA test.

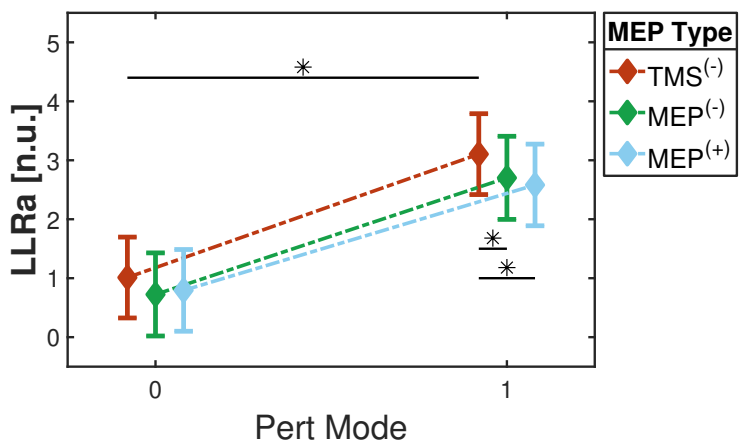

Figure 10: Effect of MEP Type and Pert Mode on the long latency response amplitude. Asterisks denote significant effects within each group.

DISCUSSION

The primary objective of this study was to determine whether *subthreshold* TMS stimulus can significantly reduce the LLRa in the FCR muscle and identify the *subthreshold* stimulus intensity and latency that resulted in the greatest reduction of the LLRa. Additionally, we wanted to determine whether the inhibitory effect was specific to the LLRa or a result of aspecific inhibition in voluntary muscle activity. We used surface EMG to record the LLR in the FCR

muscle at different levels of TMS intensity and TMS latency relative to perturbation onset. We applied *subthreshold* single pulse TMS to the left primary motor cortex to modulate corticospinal excitability during the LLR. We used a wrist robot, the MR-StretchWrist, to elicit velocity-controlled perturbations and evoke stretch responses in the FCR muscle. We found a significant effect of*subthreshold* TMS on the perturbation-evoked LLR, indicating that changes in the LLR were associated with *subthreshold* TMS application. Specifically, we found that *subthreshold* TMS latency had a significant effect on the LLRa, indicating that the ability of TMS to reduce the LLR is dependent on when the TMS pulse is applied relative to the onset of a perturbation. We found no significant effect of TMS intensity on the LLRa, suggesting that the two chosen TMS intensities (90% and 95% of the active motor threshold - AMT) result in a similar cortical inhibition when applied at a specific latency prior to perturbation onset. We confirmed the findings by restricting our analysis to *subthreshold* trials, defined on a trial-by-trial basis depending on the EMG signal measured in presence of TMS, and established that *subthreshold* TMS resulted in significant inhibition at a latency of 50 ms even when using strict thresholds for the definition of a subthreshold trial. Moreover, we found that the *subthreshold* TMS induced cortical inhibition that was not found to be LLR specific LLR.

Thus, this study establishes the inhibitory effect of *subthreshold* TMS when applied prior to perturbation onset on the LLR in the FCR muscle. Knowledge deriving from this study is crucial in understanding how *subthreshold* TMS can be used to decouple the contribution of cortical and subcortical contributions to the long-latency response and provide insight for the design of *subthreshold* TMS protocols integrated with functional neuroimaging.

Effect of TMS Latency on the Long-Latency Response

We found that cortical TMS can significantly reduce the LLR in the FCR when TMS is applied prior to perturbation onset. Specifically, we found that single-pulse TMS applied such that the hypothetical MEP peak would arrive at the muscle 20 ms or 50 ms prior to perturbation onset significantly reduced the LLRa compared to the perturbation only control. However, there was not a significant reduction in the LLRa when the hypothetical MEP peak would arrive at the muscle at 0 ms prior to perturbation onset.

Our data support the idea that the ability of single-pulse TMS to inhibit the LLR is time-dependent. Previous studies have also shown the effect of TMS on the LLR to be dependent on the timing of TMS application. *Suprathreshold* TMS significantly reduces the LLR when applied 50 ms prior to perturbation onset in both the biceps brachii and the extensor carpi radialis (42, 43). Additionally, when TMS is applied such that the MEP arrives during the SLR onset, both *subthreshold* and *suprathreshold* TMS result in a reduction in the LLRa (5). There exists a specific time-window for the TMS pulse application that results in LLR reduction (39). TMS applied too close to the LLR would not allow enough time for intracortical inhibition to occur and TMS applied too

early would led to the extinction of the silent period prior to the LLR.

This time-dependent effect of TMS can be explained by the neuromuscular delays following TMS application. There is an initial inhibition attributed to the motoneuron after-hyperpolarization of spinal origin, 50 ms to 80 ms following MEP offset (34). The later component of the silent period, 80 ms to roughly 150 ms following MEP offset, is suggested to be due to activation of GABA inhibitors which reduce the excitability of cortical motor pathways (34, 31, 49). This may explain why the LLRa reduction increased with latency and why it was greatest in the T_3 mode. In previous studies, TMS reduced the LLRa with roughly a 38.3% reduction in the biceps brachii and 32% reduction in the ECR when applied 50 ms prior to perturbation onset (42, 43). These findings align with our T_3 mode where the hypothetical MEP peak would arrive 50 ms prior to perturbation onset and results in a 37.3% EMG reduction. All this taken together, there exists a specific TMS latency window needed to overlay the cortical component of the silent period with the LLR to induce significant inhibition. Overall, we found TMS applied with a latency of 50 ms prior to the perturbation results in the greatest reduction of the LLR.

Effect of TMS Intensity on the Long-Latency Response

In this study, we found that both TMS intensities of 90% and 95% AMT resulted in a similar reduction of the LLR when applied prior to perturbation onset. From our findings, we found an overall EMG reduction of 37.3% for T_3 which aligns with the degree of inhibition observed in previous studies (40, 41, 42, 43). When applied 50 ms prior to perturbation onset, *suprathreshold* TMS reduces the LLR amplitude by 38.3% in the biceps brachii and 32% in the ECR for a stiff, do not intervene condition (42, 43). Furthermore, *suprathreshold* TMS applied at the same timing reduces the LLR modulation by 60% in the pectoralis and 31.5% in the FCR. (40, 41). When TMS is applied during the SLR onset, there is a 15% reduction in the LLR for *suprathreshold* TMS and a 43% reduction for *suprathreshold* TMS (5). However, this effect is likely due to spinal inhibition lasting approximately 50-80 ms post MEP offset.

In our study, since the difference in TMS intensities was 5% AMT, the difference may not have been large enough to cause a significant change in the degree of inhibition in the LLRa. It is suggested that higher TMS intensities would activate more inhibitory motor neurons and result in a longer silent period duration compared to lower *subthreshold* TMS intensities (50, 51, 52, 53). This may explain why with higher TMS intensities, the silent period duration increases and thus the resulting LLR reduction would be greater over a specified time period.

Additionally, we wanted to confirm whether the LLR inhibition was present when we considered trials without motor-evoked potentials. We found a significant effect of TMS when timed to arrive 50 ms prior to perturbation, even for the most strict MEP thresholding methods. These findings show that LLR inhibition is not dependent of the presence of a motor-evoked potential and confirms our results with all TMS trials. These findings agree with previous literature

that showed *subthreshold* TMS results in LLR inhibition when no facilitatory EMG activity is observed immediately following TMS (39).

The finding of a significant inhibition in LLRa was consistent across experiments.

Some TMS trials resulted in noticeable motor-evoked potentials in TMS stimulation modes defined based on a percentage of the active motor threshold. We found the most robust way to define an $MEP^{(+)}$ trial was using a threshold defined relative to the background standard deviation. Thus, it is suggested to determine the TMS intensity based on the muscle activity surpassing a threshold based on the standard deviation of background, rather than an arbitrary EMG value. Nevertheless, the finding of a significant inhibition in LLRa was consistent across thresholding methods (Fig. 8)

The finding of a significant inhibitory effect of TMS on LLR was consistent across the two coil orientations considered in this study, and held true when the coil was oriented at 90° (M-L) relative to the mid-sagittal plane (Exp 1), and when it was oriented at 45° (P-A) relative to the mid-sagittal plane (Exp 2). Qualitatively, we found a greater reduction in the LLRa with the 90° coil orientation compared to the 45° coil orientation, possibly due to the higher TMS intensities required for a given fraction of AMT when using the 90° orientation. These higher intensities may provide stimulus to a larger area surrounding the targeted M1, and result into greater intracortical inhibition, the mechanism advanced to be responsible for cortical inhibition via the silent period (54, 55).

Specificity of Cortical Inhibition

We conducted a second TMS experiment to determine whether the TMS-induced cortical inhibition was specific to the LLR. Our findings show that the LLR reduction was not significantly different than the voluntary muscle activity reduction observed during the same time period in $MEP^{(-)}$ trials, suggesting no specific LLR inhibition. However, for $MEP^{(+)}$ trials, we observed a significantly greater LLR inhibition compared to voluntary muscle activity inhibition. This suggests that *suprathreshold* TMS conditions yield LLR specific inhibition, i.e., an inhibitory effect that is larger than the one measured in absence of muscle stretch. Taken together, these findings indicate that *subthreshold* TMS inhibits a portion of the contribution of the corticospinal tract to muscle activation measured after the stimulus, while *suprathreshold* TMS also modulates the corticospinal contribution specific to LLR.

These findings are in disagreement with the previous studies who identified a inhibitory effect of TMS on LLRa (specifically, (39), (5), (38)), and established that, at least in some conditions, the TMS-induced inhibition was larger than the one measured in absence of muscle stretch (LLR-specific inhibition). It is worth noting that all the previously reported paradigms resulted in an hypothetical MEP occurring after perturbation onset, and typically before SLR onset. Given what we know about the timing of the TMS-induced silent period (34), it is reasonable to assume that these paradigms achieved LLR-specific inhibition because they aligned the TMS pulse with the phase where the induced inhibitory

effect is spinal, rather than cortical, as sought by our stimulation paradigm.

Significance for Future Work

From our results, the LLRa never completely diminishes under any *subthreshold* TMS latencies, suggesting continued supraspinal contributions during corticospinal inhibition. It has been shown that the LLR has spinal, subcortical, and cortical components (5, 6, 56, 57). This suggests that the LLRa did not completely diminish during cortical inhibition because of the sustained contribution of spinal, subcortical, or remaining cortical circuits (5). This suggests that there is a continued contribution of stretch-reflex circuits in the presence of cortical inhibition and may be independent from cortical output. Future studies need to be done to confirm the effect of cortical inhibition on subcortical structures. Such studies would allow us to investigate whether the RST can contribute to functional motor behavior during conditions of reduced corticospinal signal, possibly including those resulting from such lesions responsible for upper motor neuron syndrome. However, the clinical implications of these findings need to be confirmed in a population with corticospinal impairment. Future directions of this work involve performing this TMS protocol with functional neuroimaging to quantify the cortical and subcortical brain areas associated with *subthreshold* TMS, wrist perturbations, and LLR inhibition.

Study Limitations

This study has some limitations that should be considered in the discussion of the results. One limitation is that subjects may have moved during the experimental procedure relative to the start of the experiment. If the subject moved >4 mm or rotated >15°, movement may result in stimulating the forearm motor hot spot with a lower TMS intensity than desired result in lower cortical inhibition. Alternatively, head movements could result in a better location for stimulating the forearm motor hot spot resulting in a higher TMS intensity than desired. We tracked head movement throughout the experiment and the active motor threshold determination procedure. If the subject moved >4 mm in any direction or rotated >15° in any plane relative to the starting position and orientation, the TMS coil was re-localized to be placed over the forearm motor hotspot and the AMT was confirmed. In order to minimize subject head movement, subjects were given a chin support to support the weight of their head and keep it in position during the experiment.

Another limitation is the possibility that no stretch responses occurred in the forearm during wrist perturbations or the stretch responses were not large enough compared to background contraction activity. This could be because subjects might not have been activating their FCR muscle enough during background contraction or the velocity of the perturbation was not large enough to induce a high stretch response in that muscle. On the other hand, it is possible that some subjects could have resisted some perturbations. When resisting a perturbation, there will be a higher long-latency response then when yielding to

a perturbation. Ideally, this would not have occurred in all perturbations but may have occurred in some. This would result in the inhibitory effect of TMS not being appropriately quantified in the long-latency response amplitude. To try to minimize the potential for participants to resist perturbations, they were cued to yield to the perturbation before the start of each trial.

A third limitation in our study is the participant's body energy levels could have had an effect on how excitable their corticospinal tract was to TMS. For example, participants who drink coffee regularly would be more sensitive to TMS and have an AMT lower than they normally would without caffeine in their system. Alternatively, if participants did not get sufficient sleep or were in a fatigued state, their AMT might be higher than usual on that specific day. To account for this, we instructed participants to avoid drinking coffee or working out during the day of the experimental session. No participant verbally reported of having drunk coffee or working out prior to their data collection session.

Conclusions

The objective of this study was to determine the TMS parameters, intensity and latency relative to perturbation onset, that significantly reduced the long-latency response amplitude in the FCR muscle when applied to the motor cortex. We found that the ability of *subthreshold* TMS to reduce the LLRa depends on the latency when *subthreshold* TMS is applied prior to perturbation onset. Furthermore, during the LLR period following TMS, there remains a positive LLRa suggesting the involvement of cortical, subcortical, or spinal circuitry in generation of the LLR during reduced corticospinal tract signal. Further studies need to be done to determine the location of the cortical component of the silent period induced by TMS during the LLR. Additionally, future work needs to be conducted to determine the role of subcortical brain regions in the contribution to the LLR during the silent period. Knowledge from these studies could provide further information on how TMS modulates corticospinal excitability and how subcortical brain regions contribute to functional motor output during reduced corticospinal excitability. The findings of these studies would provide crucial information on the role of secondary motor pathways such as the reticulospinal tract on the generation of motor commands during reduced cortical input.

ACKNOWLEDGEMENTS

This research was funded by Delaware CTR ACCEL and the Delaware INBRE program.

References

[1] Peter B.C. Matthews. The human stretch reflex and the motor cortex. *Trends in Neurosciences*, 14(3):87–91, 1991.

[2] T. Sinkjaer, E. Toft, S. Andreassen, and B. C. Hornemann. Muscle stiffness in human ankle dorsiflexors: Intrinsic and reflex components. *Journal of Neurophysiology*, 60(3):1110–1121, 1988.

[3] Isaac L. Kurtzer. Long-latency reflexes account for limb biomechanics through several supraspinal pathways. *Frontiers in Integrative Neuroscience*, 8(JAN):1–19, 2015.

[4] J. Andrew Pruszynski and Stephen H. Scott. Optimal feedback control and the long-latency stretch response. *Experimental Brain Research*, 218(3):341–359, 2012.

[5] Gwyn N. Lewis, Melody A. Polych, and Winston D. Byblow. Proposed cortical and sub-cortical contributions to the long-latency stretch reflex in the forearm. *Experimental Brain Research*, 156(1):72–79, 2004.

[6] J. Andrew Pruszynski, Isaac Kurtzer, and Stephen H. Scott. The long-latency reflex is composed of at least two functionally independent processes. *Journal of Neurophysiology*, 106(1):449–459, 2011.

[7] E. Palmer and P. Ashby. Evidence that a long latency stretch reflex in humans is transcortical. *The Journal of Physiology*, 449(1):429–440, 1992.

[8] MJL Perenboom, M Van de Ruit, JH De Groot, AC Schouten, and CGM Meskers. Evidence for sustained cortical involvement in peripheral stretch reflex during the full long latency reflex period. *Neuroscience*, 584:214–218, 2015.

[9] N. Mrachacz-Kersting, M. J. Grey, and T. Sinkjær. Evidence for a supraspinal contribution to the human quadriceps long-latency stretch reflex. *Experimental Brain Research*, 168(4):529–540, 2006.

[10] Isaac L. Kurtzer, J. Andrew Pruszynski, and Stephen H. Scott. Long-Latency Reflexes of the Human Arm Reflect an Internal Model of Limb Dynamics. *Current Biology*, 18(6):449–453, 2008.

[11] C. Capaday, R. Forget, R. Fraser, and Y. Lamarre. Evidence for a contribution of the motor cortex to the long-latency stretch reflex of the human thumb. *The Journal of Physiology*, 440(1):243–255, 1991.

[12] P. D. Cheney and E. E. Fetz. Corticomotoneuronal cells contribute to long-latency stretch reflexes in the rhesus monkey. *The Journal of Physiology*, 349(1):249–272, 1984.

[13] Vaughan G. Macefield, John C. Rothwell, and Brian L. Day. The contribution of transcortical pathways to long-latency stretch and tactile reflexes in human hand muscles. *Experimental Brain Research*, 108(1):147–154, 1996.

[14] N Petersen, L O D Christensen, H Morita, T Sinkjòr, J Nielsen, Physiologisches Institut, and Christian-albrechts-universit Kiel. Tjp0512-0267. pages 267–276, 1998.

[15] Frédéric Crevecoeur and Stephen H Scott. Priors engaged in long-latency responses to mechanical perturbations suggest a rapid update in state estimation. *PLoS computational biology*, 9(8):e1003177, 2013.

[16] Robert A. Davidoff. Skeletal muscle tone and the misunderstood stretch reflex. *Neurology*, 42(5):951–963, 1992.

[17] Vengateswaran J. Ravichandran, Claire F. Honeycutt, Jonathan Shemmell, and Eric J. Perreault. Instruction-dependent modulation of the long-latency stretch reflex is associated with indicators of startle. *Experimental Brain Research*, 230(1):59–69, 2013.

[18] Jonathan Shemmell, Matthew A. Krutky, and Eric J. Perreault. Stretch sensitive reflexes as an adaptive mechanism for maintaining limb stability. *Clinical Neurophysiology*, 121(10):1680–1689, 2010.

[19] Yonas Akalu, Ashlyn K. Frazer, Glyn Howatson, Alan J. Pearce, Ummatul Siddique, Mohamad Rostami, Jamie Tallent, and Dawson J. Kidgell. Identifying the role of the reticulospinal tract for strength and motor recovery: A scoping review of nonhuman and human studies. *Physiological Reports*, 11(14):1–26, 2023.

[20] Stuart N. Baker. The primate reticulospinal tract, hand function and functional recovery. *Journal of Physiology*, 589(23):5603–5612, 2011.

[21] Adam G. Davidson and John A. Buford. Bilateral actions of the reticulospinal tract on arm and shoulder muscles in the monkey: Stimulus triggered averaging. *Experimental Brain Research*, 173(1):25–39, 2006.

[22] Demetris S Soteropoulos, Elizabeth R Williams, and Stuart N Baker. Cells in the monkey ponto-medullary reticular formation modulate their activity with slow finger movements. *The Journal of physiology*, 590(16):4011–4027, 2012.

[23] C. Nicholas Riddle, Steve A. Edgley, and Stuart N. Baker. Direct and indirect connections with upper limb motoneurons from the primate reticulospinal tract. *Journal of Neuroscience*, 29(15):4993–4999, 2009.

[24] Claire Fletcher Honeycutt, Michael Kharouta, and Eric Jon Perreault. Evidence for reticulospinal contributions to coordinated finger movements in humans. *Journal of Neurophysiology*, 110(7):1476–1483, 2013.

[25] Christopher J. Forgaard, Ian M. Franks, Kimberly Bennett, Dana Maslovat, and Romeo Chua. Mechanical perturbations can elicit triggered reactions in the absence of a startle response. *Experimental Brain Research*, 236(2):365–379, 2018.

[26] Christopher J. Forgaard, Ian M. Franks, Dana Maslovat, Laurence Chin, and Romeo Chua. Voluntary reaction time and long-latency reflex modulation. *Journal of Neurophysiology*, 114(6):3386–3399, 2015.

[27] J.C. Rothwell. The startle reflex, voluntary movement, and the reticulospinal tract. *Supplements to Clinical Neurophysiology*, 58:223–231, 2006.

[28] Andrea Zonnino, Andria J. Farrens, David Ress, and Fabrizio Sergi. Measurement of stretch-evoked brainstem function using fMRI. *Scientific Reports*, 11(1):1–21, 2021.

[29] Ulf Ziemann, Johannes Netz, Andrea Szelényi, and Volker Hömberg. Spinal and supraspinal mechanisms contribute to the silent period in the contracting soleus muscle after transcranial magnetic stimulation of human motor cortex. *Neuroscience Letters*, 156(1-2):167–171, 1993.

[30] Sergiu Groppa, Boris H. Schlaak, Alexander Münchau, Nicole Werner-Petroll, Janin Dünnweber, Tobias Bäumer, Bart F.L. van Nuenen, and Hartwig R. Siebner. The human dorsal premotor cortex facilitates the excitability of ipsilateral primary motor cortex via a short latency cortico-cortical route. *Human Brain Mapping*, 33(2):419–430, 2012.

[31] K. E. Hupfeld, C. W. Swanson, B. W. Fling, and R. D. Seidler. TMS-induced silent periods: A review of methods and call for consistency. *Journal of Neuroscience Methods*, 346(June):108950, 2020.

[32] M Inghillerj, A Berardelli, G Cruccu, and M Manfredi. Silent Period Evoked By Transcranial Stimulation of. *Journal of Physiology*, 466:521–534, 1992.

[33] B. W. Connors, R. C. Malenka, and L. R. Silva. Two inhibitory postsynaptic potentials, and GABAA and GABAB receptor-mediated responses in neocortex of rat and cat. *The Journal of Physiology*, 406(1):443–468, 1988.

[34] Jakob Škarabot, Ricardo N.O. Mesquita, Callum G. Brownstein, and Paul Ansdell. Myths and Methodologies: How loud is the story told by the transcranial magnetic stimulation-evoked silent period? *Experimental Physiology*, 104(5):635–642, 2019.

[35] K. Krnjevij, Mirjana Randiot, and D W Straughant. An Inhibitory Process in the Cerebral Cortex. *Journal of Physiology*, 184:16–48, 1966.

[36] Michelle N. McDonnell, Yuri Orekhov, and Ulf Ziemann. The role of GABAB receptors in intracortical inhibition in the human motor cortex. *Experimental Brain Research*, 173(1):86–93, 2006.

[37] Nicolas Lang, Elke Sueske, Alkomiet Hasan, Walter Paulus, and Frithjof Tergau. Pregabalin exerts oppositional effects on different inhibitory circuits in human motor cortex: A double-blind, placebo-controlled transcranial magnetic stimulation study. *Epilepsia*, 47(5):813–819, 2006.

[38] BL Day, H Riescher, A Struppler, JC Rothwell, and CD Marsden. Changes in the response to magnetic and electrical stimulation of the motor cortex following muscle stretch in man. *The Journal of physiology*, 433(1):41–57, 1991.

[39] Johan Van Doornik, Yoshihisa Masakado, Thomas Sinkjaer, and Jens Bo Nielsen. The suppression of the long-latency stretch reflex in the human tibialis anterior muscle by transcranial magnetic stimulation. *Experimental Brain Research*, 157(3):403–406, 2004.

[40] Toshitaka Kimura, Patrick Haggard, and Hiroaki Gomi. Transcranial magnetic stimulation over sensorimotor cortex disrupts anticipatory reflex gain modulation for skilled action. *Journal of Neuroscience*, 26(36):9272–9281, 2006.

[41] L. Spieser, S. Aubert, and M. Bonnard. Involvement of SMAp in the intention-related long latency stretch reflex modulation: A TMS study. *Neuroscience*, 246:329–341, 2013.

[42] Jonathan Shemmell, Hi An Je, and Eric J. Perreault. The differential role of motor cortex in stretch reflex modulation induced by changes in environmental mechanics and verbal instruction. *Journal of Neuroscience*, 29(42):13255–13263, 2009.

[43] Jonathan Fox and Jonathan Shemmell. The ipsilateral motor cortex does not contribute to long-latency stretch reflex amplitude at the wrist. *Brain and Behavior*, 4(1):60–69, 2014.

[44] Hadj Boumediene Meziane, Laure Spieser, Jean Pailhous, and Mireille Bonnard. Corticospinal control of wrist muscles during expectation of a motor perturbation: A trasncranial magnetic stimulation study. *Behavioural Brain Research*, 198:459–465, 2009.

[45] L. Spieser, H. B. Meziane, and M. Bonnard. Cortical mechanisms underlying stretch reflex adaptation to intention: A combined EEG-TMS study. *NeuroImage*, 52(1):316–325, 2010.

[46] Jane E. Butler, Nicolas C. Petersen, Robert D. Herbert, Simon C. Gandevia, and Janet L. Taylor. Origin of the low-level EMG during the silent period following transcranial magnetic stimulation. *Clinical Neurophysiology*, 123(7):1409–1414, 2012.

[47] A. Pascual-Leone, L. G. Cohen, J. P. Brasil-Neto, and M. Hallett. Noninvasive differentiation of motor cortical representation of hand muscles by mapping of optimal current directions. *Electroencephalography and Clinical Neurophysiology/ Evoked Potentials*, 93(1):42–48, 1994.

[48] Lars Richter, Gunnar Neumann, Stephen Oung, Achim Schweikard, and Peter Trillenberg. Optimal coil orientation for transcranial magnetic stimulation. *PloS one*, 8(4):e60358, 2013.

[49] S. A. Wilson, R. J. Lockwood, G. W. Thickbroom, and F. L. Mastaglia. The muscle silent period following transcranial magnetic cortical stimulation. *Journal of the Neurological Sciences*, 114(2):216–222, 1993.

[50] King Hee Ho, Kannan Nithi, and Kerry R. Mills. Covariation between human intrinsic hand muscles of the silent periods and compound muscle action potentials evoked by magnetic brain stimulation: Evidence for common inhibitory connections. *Experimental Brain Research*, 122(4):433–440, 1998.

[51] Janet L. Taylor, Gabrielle M. Allen, Jane E. Butler, and S. C. Gandevia. Effect of contraction strength on responses in biceps brachii and adductor pollicis to transcranial magnetic stimulation. *Experimental Brain Research*, 117(3):472–478, 1997.

[52] V. Di Lazzaro, D. Restuccia, A. Oliviero, P. Profice, L. Ferrara, A. Insola, P. Mazzone, P. Tonali, and J. C. Rothwell. Magnetic transcranial stimulation at intensities below active motor threshold activates intracortical inhibitory circuits. *Experimental Brain Research*, 119(2):265–268, 1998.

[53] Ulf Ziemann, John C. Rothwell, and Michael C. Ridding. Interaction between intracortical inhibition and facilitation in human motor cortex. *Journal of Physiology*, 496(3):873–881, 1996.

[54] Carlo Trompetto, Alessandro Buccolieri, Lucio Marinelli, and Giovanni Abbruzzese. Differential modulation of motor evoked potential and silent period by activation of intracortical inhibitory circuits. *Clinical Neurophysiology*, 112(10):1822–1827, 2001.

[55] JP Brasil-Neto, A Cammarota, J Valls-Solé, A Pascual-Leone, M Hallett, and LG Cohen. Role of intracortical mechanisms in the late part of the silent period to transcranial stimulation of the human motor cortex. *Acta neurologica scandinavica*, 92(5):383–386, 1995.

[56] Gwyn N. Lewis, Colum D. MacKinnon, and Eric J. Perreault. The effect of task instruction on the excitability of spinal and supraspinal reflex pathways projecting to the biceps muscle. *Experimental Brain Research*, 174(3):413–425, 2006.

[57] Colum D. MacKinnon, Mary C. Verrier, and William G. Tatton. Motor cortical potentials precede long-latency EMG adivity evoked by imposed displacements of the human wrist. *Experimental Brain Research*, 131(4):477–490, 2000.

Supplementary Materials

Supplementary Methods

Subject-level LLR analysis

For each subject, we first used the Shapiro-Wilcoxon test to determine if the normalized LLRa dataset was normally distributed. Because the test highlighted that the LLRa data for each subject was non-normally distributed, nonparametric tests were used for statistical analysis.

Subject-level statistical analysis was performed using the Wilcoxon test, and post-hoc tests were performed using the Steel method, setting the TMS off – Pert On mode as the control mode while controlling for multiple comparisons (4 per subject). As an outcome of this analysis, we counted the number of subjects that had a significant difference from control

All statistical analyses reported above were performed using JMP Pro Version 16.2.0 (SAS Institute Inc., Cary, NC, United States).

Time series analysis

A 1-D time series ANOVA was performed on the normalized FCR EMG for each subject from 100 ms before perturbation onset to 150 ms after perturbation onset using the SPM 1D software package (Pataky et al., 2015, 2016). While the 0D statistical tests focused on the effect of TMS timing and intensity on the LLRa over a specific time period, a 1D statistical tests allowed us to determine the effect of TMS timing and intensity on the normalized EMG response over the entire time period while accounting for multiple comparisons.

We performed a two-way model to test the effects of two factors, TMS mode, TMS intensity, and their interaction, on the normalized EMG response using the function `anova2onerm`. This test accounted for the random effect of subject ID and accounted for the repeated measures factor of TMS modes. Also, a 1-way rmANOVA was performed with all subjects to determine the effect of TMS mode for the entire stretch reflex response period. In each model, TMS mode had four levels: T_1, T_2, T_3, and PertOnly as the control mode. The measurements in the Back Only mode were not included in the analysis because the rmANOVA package currently assumes equal variances between conditions, and would lead to under-estimating the variance of the whole dataset in presence of EMG data measured in the Background Only mode (no stimulus response). Random factors in the rmANOVA model were subject ID, and the software automatically estimated terms for both subject and for the interaction between subject and TMS mode.

We performed two-sided paired t-tests for 1D post-hoc analysis to determine which TMS mode levels had a significantly different EMG response than the control. Post-hoc analysis was performed by comparing T_1, T_2, or T_3 with the control mode (PertOnly) to determine which TMS modes were significantly different at each time point (100ms prior to 150 ms post perturabation onset). The two-sided paired t-test were performed with the normalized FCR EMG

response for each condition for all subjects. We used a bonferroni-corrected α value of 0.017 in the t-tests to accounted for the multiple comparisons that were performed. The averaged normalized FCR EMG response for all subjects was plotted for visualization purposes.

The one-way rmANOVA for the effect of TMS mode was repeated for each TMS intensity group. Again, TMS mode (levels: T_1, T_2, T_3, and PertOnly) was the fixed effect, with PertOnly as the control mode. Subject ID was used as a random effect and the software automatically estimated terms for both subject and for the interaction between subject and TMS mode. Again, post-hoc analysis was performed with two-sided paired t-tests to determine which TMS modes were significantly different from the control mode at each time point. We used a bonferroni-corrected α value of 0.017 in the t-tests to accounted for the multiple comparisons that were performed.

Supplementary Results

Subject-level analysis

From the Shapiro-Wilcoxon test for normality, the LLRa data was non-normally distributed for all subjects. For the 90% AMT intensity, a significant effect of TMS mode was found in 5 out of 12 subjects for T_1, 3 out of 12 subjects for T_2, and 7 out of 12 subjects for T_3 compared to the Pert Only mode. For the 95% AMT intensity, a significant effect of TMS mode was found in 4 out of 12 subjects for T_1, 5 out of 12 subjects for T_2, and 8 out of 12 subjects for T_3 compared to the Pert Only mode. For the Back Only mode, 11 out of 12 subjects in the 90% AMT group and 10 out of 12 subjects in 95% AMT group had a significant effect compared to Pert Only mode. In subjects without a significant difference from background, the evoked muscle stretches might not have induced a large enough LLR.

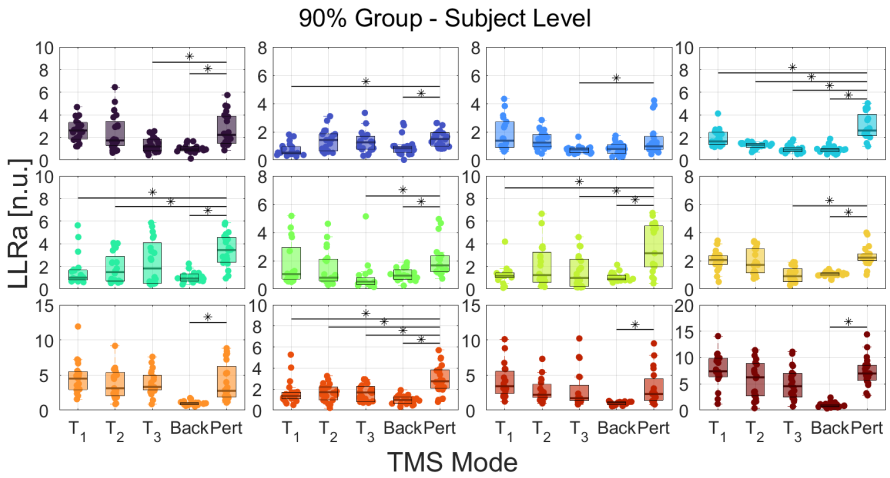

Figure S1: Subject-level results of the effect of TMS mode on the normalized long-latency response amplitude (LLRa) for the 90% AMT intensity group. Each panel represents the response from one subject. In each boxplot, the median is indicated via a horizontal line, the box extends to the 25th and 75th precentiles, and the whiskers extend to the most extreme datapoint not considered outliers (more than 2.7 standard deviations away from the mean for normally distributed data). Subject measurements of normalized LLRa for each trial are plotted as dots. Conditions that are significantly different from the Pert condition are indicated with an asterisk. The significance threshold is 0.05, corrected using the Steel's method.

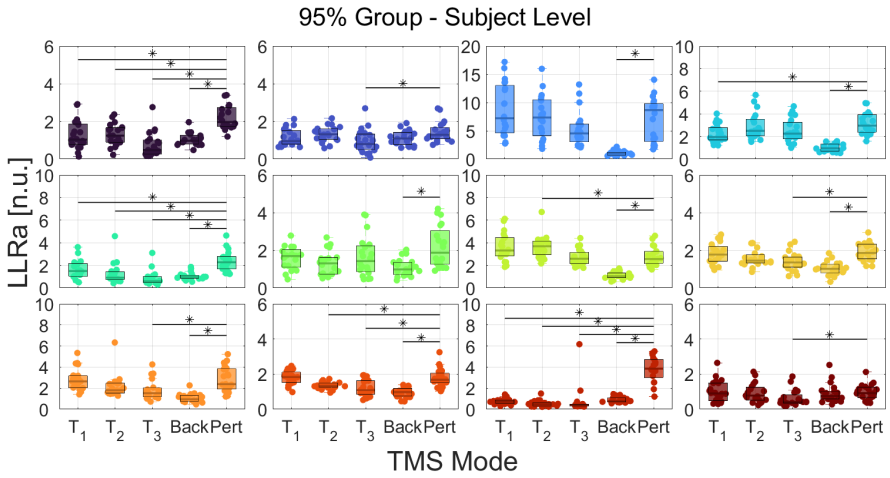

Figure S2: Subject-level results of the effect of TMS mode on the normalized long-latency response amplitude (LLRa) for the 95% AMT intensity group.

Time series analysis

The two-way repeated measures ANOVA revealed that TMS mode had a significant effect on the normalized EMG response prior to perturbation onset, immediately before and after perturbation onset, and during the LLR period. Specifically, there were significant intervals observed from -74.0ms to -38.2ms, -30.7ms to 13.7ms, and 64.1ms to 105.6ms relative to perturbation onset (local peaks at t=-59.0 ms, F=20.5; t=-25.1 ms, F=13.8; t=4.7 ms, F=14.7;and t=81.5 ms, F=20.5, respectively). There were no significant intervals from the time series analysis for the factors of TMS intensity (I) and the interaction between TMS intensity and TMS mode (I·T). Because the TMS stimuli were delivered at different times relative to perturbation onset in the different conditions, post-hoc analysis was performed on TMS modes, individually, to further break down the levels that resulted in significant differences.

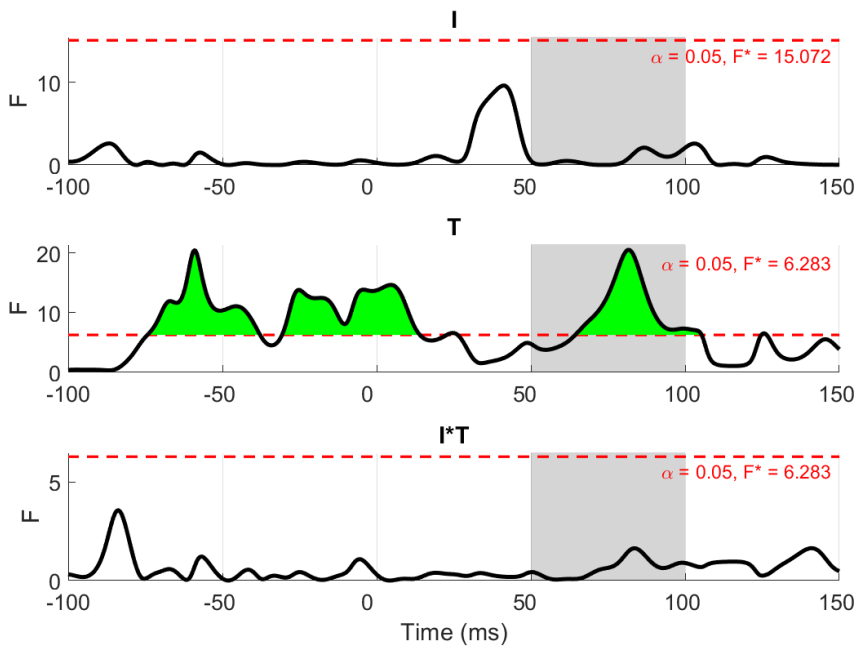

Figure S3: Time series Analysis - Two-way ANOVA for the effect of TMS Intensity (I), TMS mode (T), and their interaction (I*T) on the normalized EMG response from -100ms to 150ms relative to perturbation onset for all subjects. Alpha value is equal to 0.05. The F ratio threshold is indicated by the horizontal red line and the threshold value is given at the top right of each plot.

In T_1 TMS mode, the EMG response significantly increased prior to the LLR period from -23.8ms to 29.8ms (local peak at t=-7.8 ms, T=12.0), reflecting the excitatory effect of TMS stimulation. The EMG response significantly decreased

during the LLR period from 79.4ms to 86.8ms (local peak at t=83.0 ms, T=-4.1) and during voluntary response from 134.4 ms to 150.0 ms (local peak at t=150.0 ms, T=-4.1). The T_2 TMS mode significantly increased the EMG response prior to the LLR period from -52.8ms to 10.8ms (local peak at t=-26.8 ms, T=12.2). In T_2 TMS mode, EMG response significantly decreased during the LLR period from 53.8 ms to 92.0 ms (local peak at t=82.0 ms, T=-6.51) and during the voluntary response from 97.4 ms to 104.8 ms (local peak at t=101.0 ms, T=-4.60). In the T_3 TMS mode, the EMG response was significantly increased prior to perturbation onset, from -78.0 ms to -16.0 ms (local peak at t=-58.2 ms, T=13.1). The EMG response was significantly decreased during and after the LLR period, from 34.2 ms to 150 ms (local peaks at t=82.6 ms, T=-11.71).

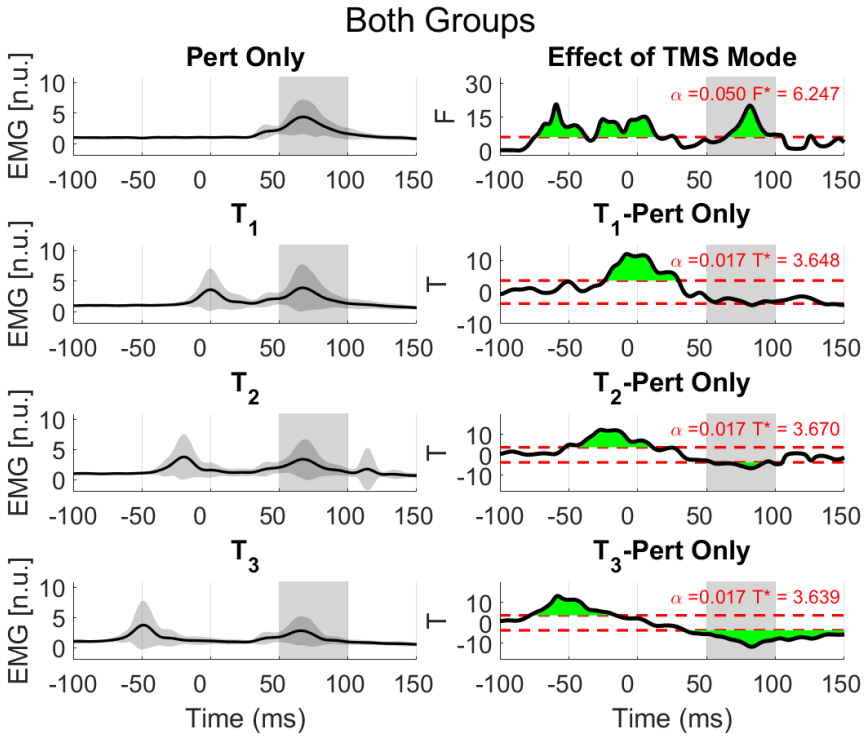

Figure S4: Time series Analysis - One-way rmANOVA for the effect of TMS mode with post-hoc tests from -100 ms to 150 ms relative to perturbation onset for all subjects. Group mean normalized EMG responses for each TMS mode are displayed on the left panels. The F scores for the effect of TMS mode are displayed on the top right panel for each time point. T test scores resulting from post-hoc time series pairwise comparisons between each TMS mode and the control mode (PertOnly) are displayed on the right bottom three panels.

For the 90% AMT intensity, from the one-way rmANOVA for the effect

of TMS mode, TMS mode had a significant effect on the normalized EMG response prior to perturbation onset, during the LLR period, and during the voluntary response period. Specifically, TMS mode had a significant effect from -61.2 ms to -56.2 ms, 75.7 ms to 87.3 ms, and 134.0 ms to 148.8 ms relative to perturbation onset (local peaks at t=-59.0 ms, F=10.2; t=81.7 ms, F=11.9; t=143.2 ms, F=10.0, respectively).

From the time series post-hoc analysis, the normalized EMG response significantly increased in T_1 prior to the LLR period, from -23.4 ms to 27.4 ms (local peak at t=-8.2 ms, T=8.6) and significantly decreased during voluntary response from 136.6 ms to 145.0 ms (local peak at t=139.8 ms, T=-3.9). In the T_2 mode, EMG response was significantly increased prior to the LLR period from -41.2 ms to 6.2 ms (local peak at t=-27.4ms, T=8.61). EMG responses significantly decreased during and after the LLR period from 70.2 ms to 86.6 ms and 134.2 ms to 147.4 ms (local peaks t=76.4 ms, T=-4.6; t=141.4 ms, T=-4.4, respectively). In the T_3 mode, the EMG response significantly increased prior to perturbation onset from -74.4ms to -14.0ms (local peak at t=-58.6 ms, T=9.5) and significantly decreased during the LLR period, from 54.6 ms to 150.0 ms (local peak at t=82.2 ms, T=-9.3).

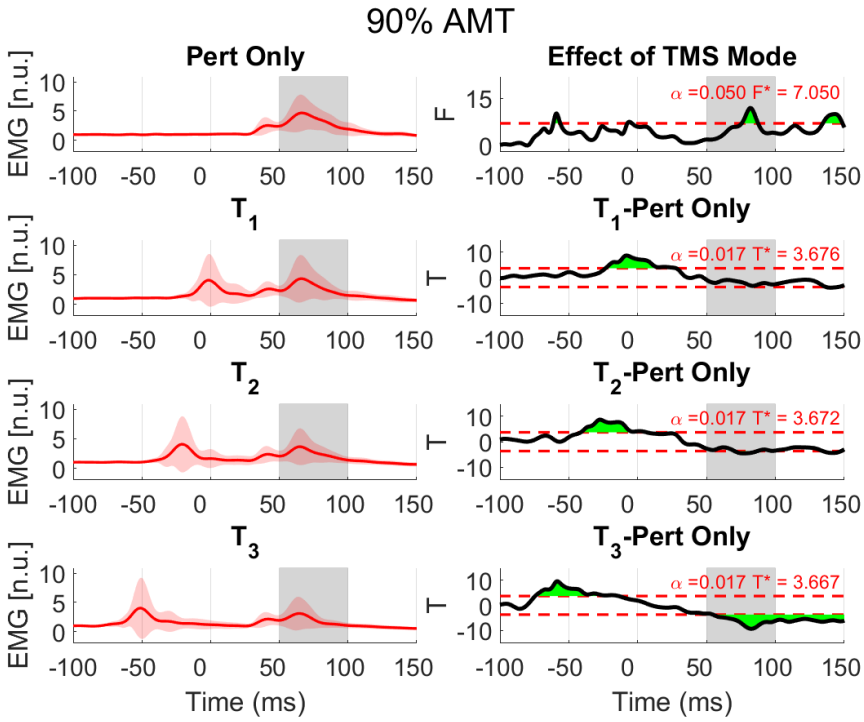

Figure S5: Time series Analysis - One-way rmANOVA for the effect of TMS mode in the 90% AMT group with post-hoc tests from -100ms to 150ms relative to perturbation onset. Group mean normalized EMG response for each TMS mode are displayed on the left panels. The F scores for the effect of TMS mode are displayed on the top right panel for each time point. T test scores resulting from post-hoc time series pairwise comparisons between each TMS mode and the control mode (PertOnly) are displayed on the right bottom three panels.

For the 95% AMT intensity, from the one-way rmANOVA, TMS mode had a significant effect on the normalized EMG response prior to perturbation onset and during the LLR period. Specifically, TMS mode had a significant effect from -67.6 ms to -46.0 ms, -27.8 ms to -15.0 ms, and -5.4 ms to 7.6 ms relative to perturbation onset (local peaks at t=-54.0 ms, F=17.3; t=-24.0 ms, F=12.6; t=-0.9 ms, F=10.4, respectively). EMG response was significantly modulated during the LLR period, 75.8 ms to 90.0 ms (local peak at t=79.9 ms, F=8.95).

From the time series post-hoc analysis, the normalized EMG response significantly increased in T_1 prior to the LLR period, from -20.2 ms to 27.8 ms (local peak at t=-1.0 ms, T=11.8). In the T_2 mode, EMG response was significantly increased prior to the LLR period from -54.6 ms to -45.0 ms and -41.8 ms to 8.6 ms (local peak at t=-50.8ms, T=5.4; t=-21.8ms, T=11.2, respectively). In the T_2 mode, EMG response was significantly decreased during the LLR period from 58.8 ms to 65.5 ms and 77.6 ms to 89.4 ms, and during the voluntary

response from 103 ms to 103.4 ms (local peak at t=62.4 ms, T=-4.3; t=83.6 ms, T=-5.6; t=103.2 ms, T=-3.7, respectively). In the T_3 mode, the EMG response significantly increased prior to perturbation onset from -83.6 ms to -76.4 ms and -69.2 ms to -24.0 ms (local peaks at t=-80.4 ms, T=4.2; t=-53.4 ms, T=13.5), and significantly decreased during the LLR period, from 35.2 ms to 130.6ms (local peak at t=83.2 ms, T=-7.4).

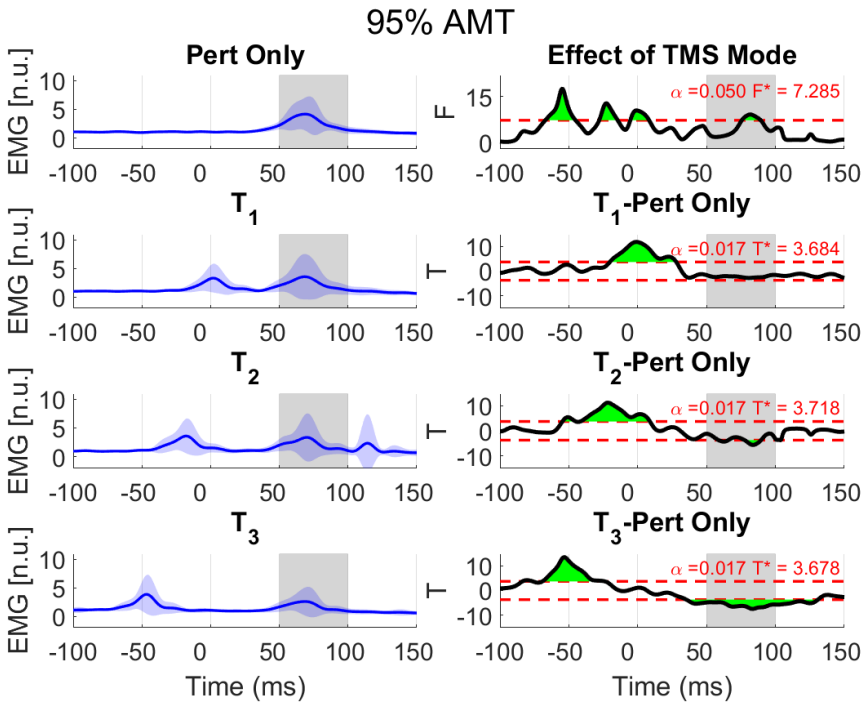

Figure S6: Time series Analysis - One-way rmANOVA for the effect of TMS mode in the 95% AMT group with post-hoc tests from -100ms to 150ms relative to perturbation onset. Group mean normalized EMG response for TMS mode plotted on the left. The F scores for each time point of the effect of TMS mode are displayed plotted on the top right. Post-hoc time series analysis results for each TMS mode compared to the control mode (PertOnly) plotted on the right bottom three panels.

Participant ID	$MEP^{(-)}$ Trials	$MEP^{(+)}$ Trials
01	11	49
02	48	12
03	19	41
04	3	57
05	8	52
06	44	16
07	48	12
08	55	5
09	29	31
10	42	18
11	0	60
12	1	59
13	5	55
14	0	60
15	46	14
16	45	15
17	25	35
18	39	21
19	49	11
20	17	43
21	51	9
22	0	60
23	0	60
24	11	49

Table S1: TMS Experiment 1 - MEP Trial Classification by participant for 1x standard deviation thresholding.

Participant ID	$MEP^{(-)}$ $Trial^{(-)}$s	$MEP^{(+)}$ Trials
01	35	15
02	6	44
03	36	14
04	0	50
05	37	13
06	0	50
07	26	24
08	18	32
09	36	14
10	21	29
11	46	4
12	0	50

Table S2: TMS Experiment 2 - MEP Trial Classification by participant for 1x standard deviation thresholding.

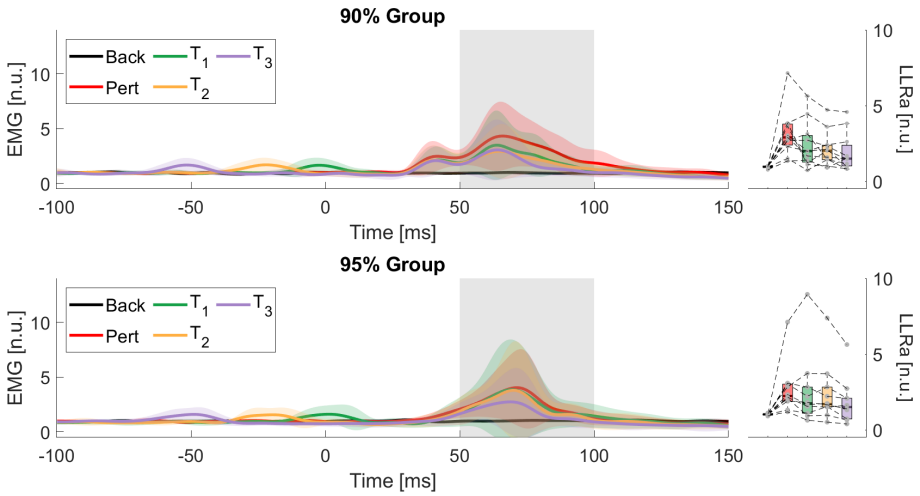

Figure S7: TMS Experiment 1 Time series normalized EMG Plots - Group mean normalized EMG responses for each TMS mode are displayed from -100 ms to 150 ms relative to perturbation onset for all subjects. The long latency response amplitudes (LLRa) for each TMS mode are displayed and broken down by TMS group. Each dot denotes the within subject average for that TMS mode. The middle line is the median of the distribution with the box ends indicating the 25% - 75% IQR. Whiskers extend out to the furthest datapoint that is not considered an outlier. Trials with EMG peaks during the expected MEP window greater than 3X standard deviation from background were excluded in this analysis

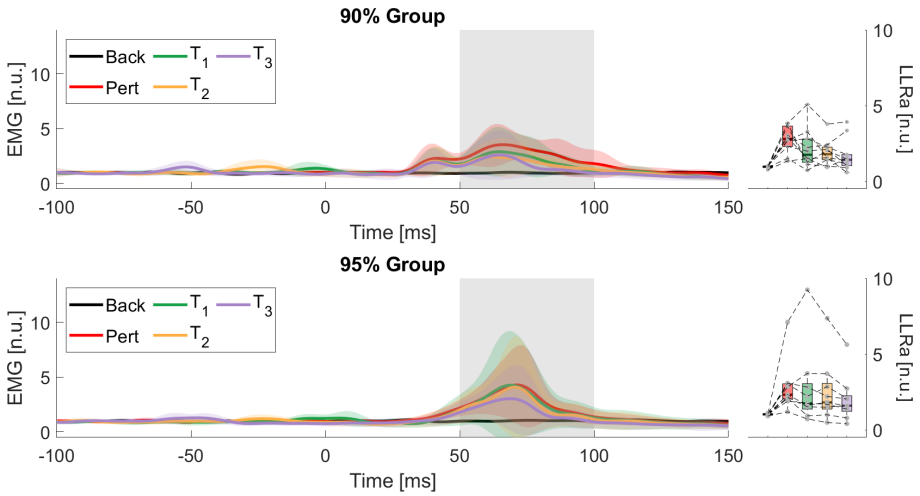

Figure S8: TMS Experiment 1 Time series normalized EMG Plots - Group mean normalized EMG responses for each TMS mode are displayed from -100 ms to 150 ms relative to perturbation onset for all subjects. The long latency response amplitudes (LLRa) for each TMS mode are displayed and broken down by TMS group. Each dot denotes the within subject average for that TMS mode. The middle line is the median of the distribution with the box ends indicating the 25% - 75% IQR. Whiskers extend out to the furthest datapoint that is not considered an outlier. Trials with EMG peaks during the expected MEP window greater than 2X standard deviation from background were excluded in this analysis.

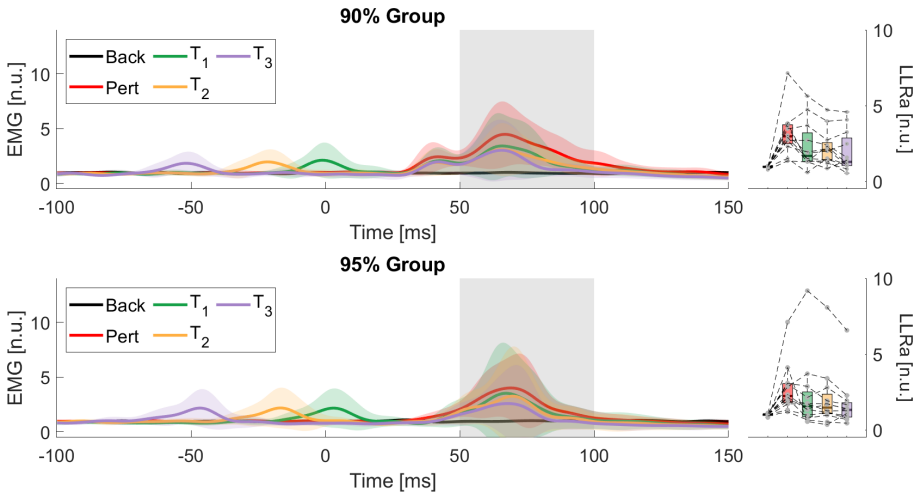

Figure S9: TMS Experiment 1 Time series normalized EMG Plots - Group mean normalized EMG responses for each TMS mode are displayed from -100 ms to 150 ms relative to perturbation onset for all subjects. The long latency response amplitudes (LLRa) for each TMS mode are displayed and broken down by TMS group. Each dot denotes the within subject average for that TMS mode. The middle line is the median of the distribution with the box ends indicating the 25% - 75% IQR. Whiskers extend out to the furthest datapoint that is not considered an outlier. Trials with EMG peaks during the expected MEP window greater than median EMG peak were excluded in this analysis.

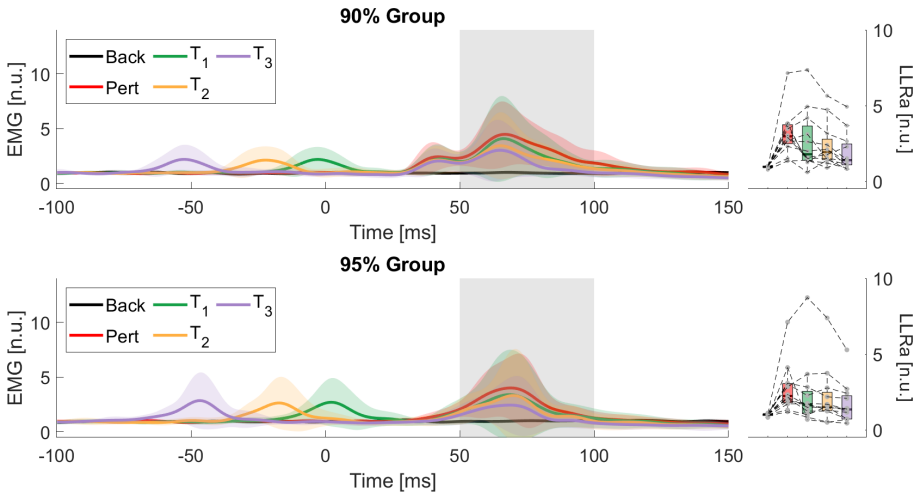

Figure S10: TMS Experiment 1 Time series normalized EMG Plots - Group mean normalized EMG responses for each TMS mode are displayed from -100 ms to 150 ms relative to perturbation onset for all subjects. The long latency response amplitudes (LLRa) for each TMS mode are displayed and broken down by TMS group. Each dot denotes the within subject average for that TMS mode. The middle line is the median of the distribution with the box ends indicating the 25% - 75% IQR. Whiskers extend out to the furthest datapoint that is not considered an outlier. Trials with EMG peaks during the expected MEP window greater than 200uV were excluded in this analysis.

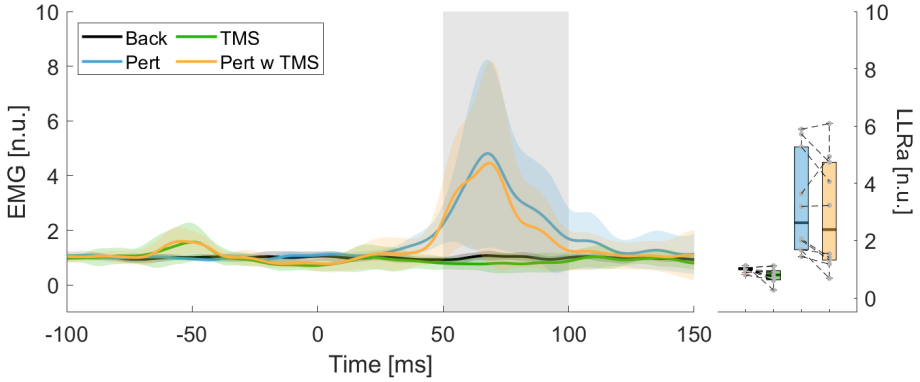

Figure S11: (Left) TMS Experiment 2 time series normalized EMG Plots - Group mean normalized EMG responses for each TMS mode are displayed from -100 ms to 150 ms relative to perturbation onset for all subjects. (Right) Normalized LLR amplitudes for each TMS mode with the datapoints plotted to show the within subject mean. The center mark indicates the median and the 25th and 75th quartile ranges are plotted with the solid boxes. The whiskers extend out to the furtherest datapoint that is not considered an outlier. Trials with EMG peaks during the expected MEP window greater than 3X standard deviation from the background EMG signal were excluded in this analysis.

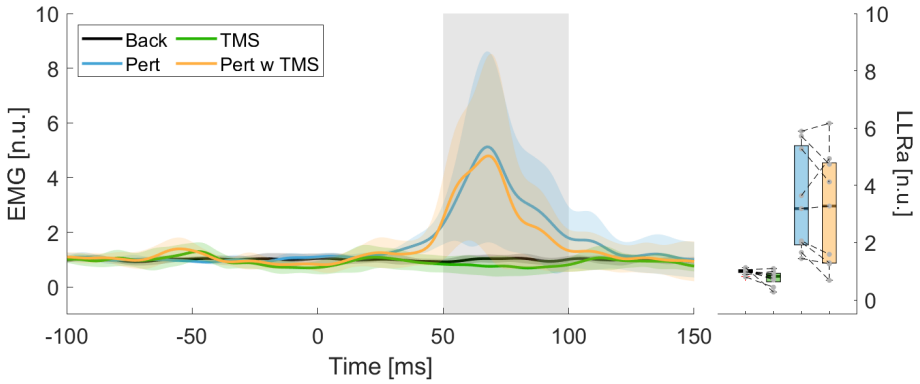

Figure S12: (Left) TMS Experiment 2 time series normalized EMG Plots - Group mean normalized EMG responses for each TMS mode are displayed from -100 ms to 150 ms relative to perturbation onset for all subjects. (Right) Normalized LLR amplitudes for each TMS mode with the datapoints plotted to show the within subject mean. The center mark indicates the median and the 25th and 75th quartile ranges are plotted with the solid boxes. The whiskers extend out to the furtherest datapoint that is not considered an outlier. Trials with EMG peaks during the expected MEP window greater than 2X standard deviation from the background EMG signal were excluded in this analysis.

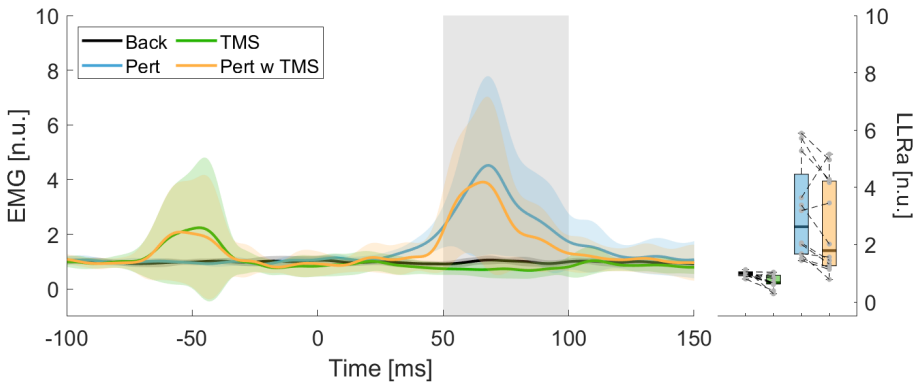

Figure S13: (Left) TMS Experiment 2 time series normalized EMG Plots - Group mean normalized EMG responses for each TMS mode are displayed from -100 ms to 150 ms relative to perturbation onset for all subjects. (Right) Normalized LLR amplitudes for each TMS mode with the datapoints plotted to show the within subject mean. The center mark indicates the median and the 25th and 75th quartile ranges are plotted with the solid boxes. The whiskers extend out to the furtherest datapoint that is not considered an outlier. Trials with EMG peaks during the expected MEP window greater than the median MEP peak were excluded in this analysis.

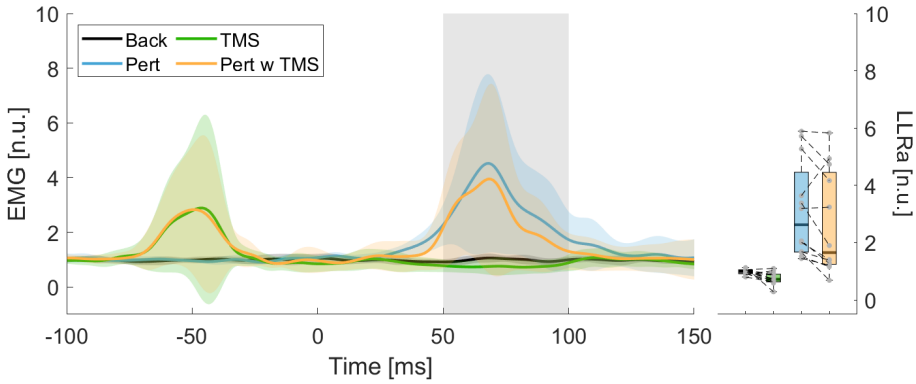

Figure S14: (Left) TMS Experiment 2 time series normalized EMG Plots - Group mean normalized EMG responses for each TMS mode are displayed from -100 ms to 150 ms relative to perturbation onset for all subjects. (Right) Normalized LLR amplitudes for each TMS mode with the datapoints plotted to show the within subject mean. The center mark indicates the median and the 25th and 75th quartile ranges are plotted with the solid boxes. The whiskers extend out to the furtherest datapoint that is not considered an outlier. Trials with EMG peaks during the expected MEP window greater than 200μV were excluded in this analysis.

Inhibitory Effect of Subthreshold TMS on the LLR in the FCR

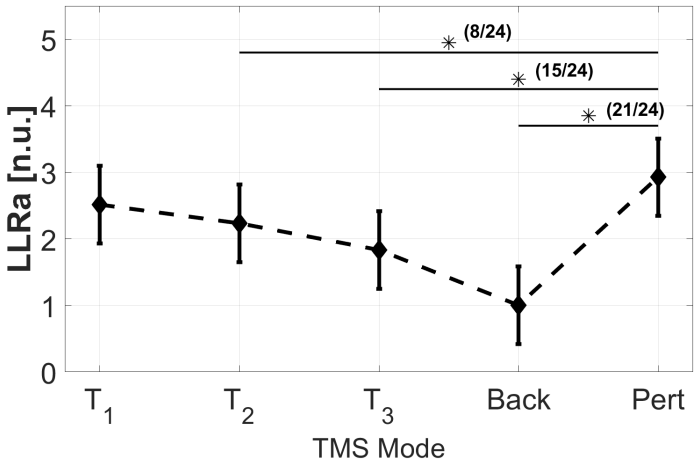

Figure S15: Effects of TMS mode the long latency response amplitude (LLRa) pooled in both groups. Asterisks denote significant effects at the group level, and numbers in parenthesis indicate the number of subjects for which that effect was detected.

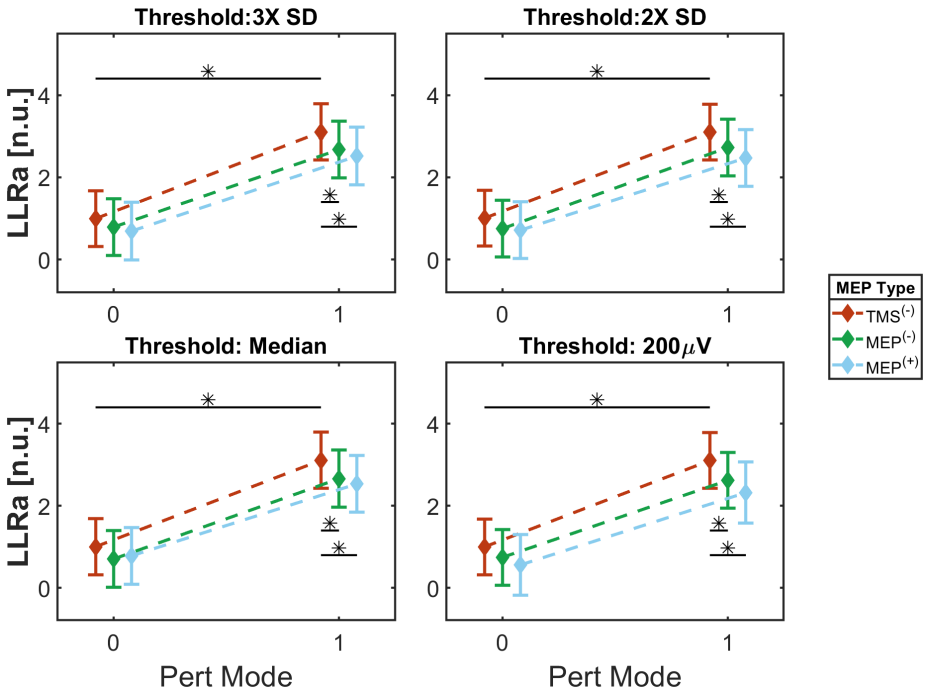

Figure S16: TMS Experiment 2 mixed model results with different MEP peak thresholding methods. Effect of MEP Type and Pert Mode on the long latency response amplitude. Asterisks denote significant effects within each group.

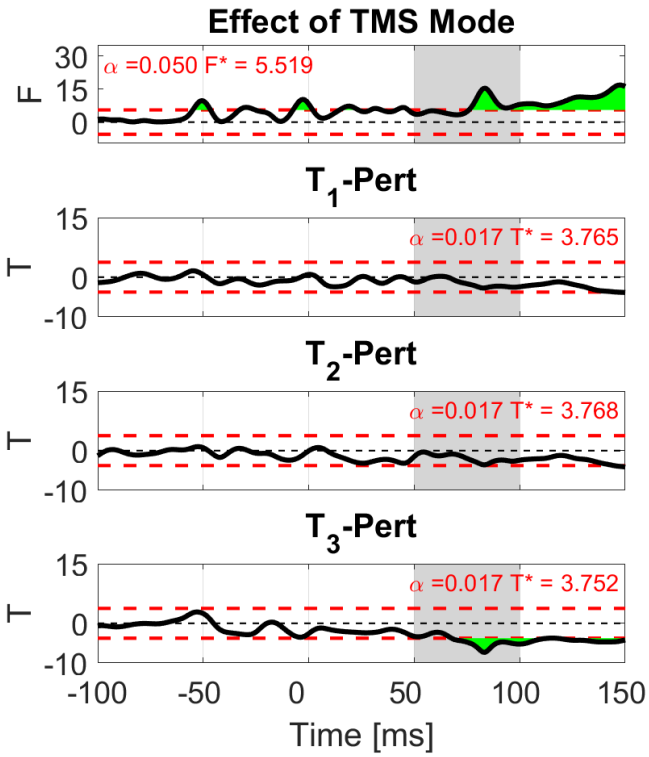

Figure S17: TMS Experiment 1 time series analysis - One-way rmANOVA for the effect of TMS mode for combined groups with low MEP trials only (<1X standard deviation) with post-hoc tests from -100ms to 150ms relative to perturbation onset. The F scores for the effect of TMS mode are displayed on the top right panel for each time point. T test scores resulting from post-hoc time series pairwise comparisons between each TMS mode and the control mode (Pert) are displayed on the right bottom three panels.

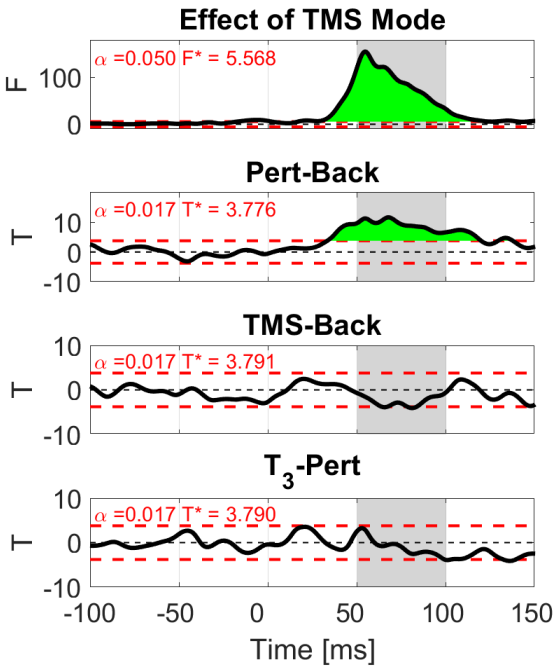

Figure S18: TMS Experiment 2 time series analysis on the low MEP trials only (<1X standard deviation). The F scores for the effect of TMS mode are displayed on the top right panel for each time point. T test scores resulting from post-hoc time series pairwise comparisons between each TMS mode and the control mode are displayed on the right bottom three panels